Pretargeting: A Path Forward for Radioimmunotherapy

Sarah M. Cheal*[1], Sebastian K. Chung*[2], Brett A. Vaughn*[1], Nai-Kong V. Cheung[3], and Steven M. Larson[1,4]

[1]*Molecular Pharmacology Program, Memorial Sloan Kettering Cancer Center, New York, New York;* [2]*Department of Surgery, Memorial Sloan Kettering Cancer Center, New York, New York;* [3]*Department of Pediatrics, Memorial Sloan Kettering Cancer Center, New York, New York; and* [4]*Department of Radiology, Memorial Sloan Kettering Cancer Center, New York, New York*

Learning Objectives: On successful completion of this activity, participants should be able to describe (1) the current status of radioimmunotherapy of human tumors with radioimmunoconjugates; (2) the concept of pretargeted radioimmunotherapy and successes/failures in clinical trials; (3) recent efforts to optimize pretargeted radioimmunotherapy, including the development of novel pretargeting systems; and (4) the future outlook for pretargeted radioimmunotherapy, including clinical trials on the horizon.

Financial Disclosure: Drs. Cheal, Cheung, and Larson are listed as coinventors on multiple patents related to this work owned by MSKCC, some of which are licensed to Y-mAbs Therapeutics, Inc. Dr. Cheal receives royalties from Y-mAbs Therapeutics Inc. Dr. Cheung receives investment interest in Y-mAbs Therapeutics, Inc., and Abpro Labs; is a consultant/advisor to Eureka Therapeutics; receives royalties from Biotec Pharmacon/Lallemand; and receives sponsored research support from Y-mAbs Therapeutics, Inc. Dr. Larson receives commercial research grants from Y-mAbs Therapeutics Inc., Genentech, Inc., Wilex AG, Telix Pharmaceuticals Limited, and Regeneron Pharmaceuticals, Inc.; holds ownership interest/equity in Voreyda Theranostics Inc. and Elucida Oncology Inc.; holds stock in ImaginAb, Inc., and Y-mAbs Therapeutics, Inc.; is the inventor and owner of issued patents both currently unlicensed and licensed by MSKCC to Samus Therapeutics, Inc., Y-mAbs Therapeutics Inc., and Elucida Oncology, Inc.; and serves as a consultant to Cynvec LLC, Eli Lilly & Co., Prescient Therapeutics Limited, Advanced Innovative Partners, LLC, Gerson Lehrman Group, Progenics Pharmaceuticals, Inc., Bristol Myers Squib, and Janssen Pharmaceuticals, Inc. The authors of this article have indicated no other relevant relationships that could be perceived as a real or apparent conflict of interest.

CME Credit: SNMMI is accredited by the Accreditation Council for Continuing Medical Education (ACCME) to sponsor continuing education for physicians. SNMMI designates each *JNM* continuing education article for a maximum of 2.0 AMA PRA Category 1 Credits. Physicians should claim only credit commensurate with the extent of their participation in the activity. For CE credit, SAM, and other credit types, participants can access this activity through the SNMMI website (http://www.snmmilearningcenter.org) through September 2025.

Pretargeted radioimmunodiagnosis and radioimmunotherapy aim to efficiently combine antitumor antibodies and medicinal radioisotopes for high-contrast imaging and high–therapeutic-index (TI) tumor targeting, respectively. As opposed to conventional radioimmunoconjugates, pretargeted approaches separate the tumor-targeting step from the payload step, thereby amplifying tumor uptake while reducing normal-tissue exposure. Alongside contrast and TI, critical parameters include antibody immunogenicity and specificity, availability of radioisotopes, and ease of use in the clinic. Each of the steps can be optimized separately; as modular systems, they can find broad applications irrespective of tumor target, tumor type, or radioisotopes. Although this versatility presents enormous opportunity, pretargeting is complex and presents unique challenges for clinical translation and optimal use in patients. The purpose of this article is to provide a brief historical perspective on the origins and development of pretargeting strategies in nuclear medicine, emphasizing 2 protein delivery systems that have been extensively evaluated (i.e., biotin–streptavidin and hapten-bispecific monoclonal antibodies), as well as radiohaptens and radioisotopes. We also highlight recent innovations, including pretargeting with bioorthogonal chemistry and novel protein vectors (such as self-assembling and disassembling proteins and Affibody molecules). We caution the reader that this is by no means a comprehensive review of the past 3 decades of pretargeted radioimmunodiagnosis and pretargeted radioimmunotherapy. But we do aim to highlight major developmental milestones and to identify benchmarks for success with regard to TI and toxicity in preclinical models and clinically. We believe this approach will lead to the identification of key obstacles to clinical success, revive interest in the utility of radiotheranostics applications, and guide development of the next generation of pretargeted theranostics.

Received Mar. 28, 2022; revision accepted Jun. 7, 2022.
For correspondence or reprints, contact Sarah M. Cheal (cheals@mskcc.org).
*Contributed equally to this work.

Key Words: general oncology; radionuclide therapy; radiopharmaceuticals; multistep; pretargeted radioimmunotherapy; radioimmunotherapy

J Nucl Med 2022; 63:1302–1315
DOI: 10.2967/jnumed.121.262186

Monoclonal antibodies (mAbs) are attractive vehicles for delivering cytotoxic payloads to tumors using cell-surface targets as ZIP codes. However, the complexity of the tumor microenvironment and the pharmacokinetics of mAbs in vivo have created major hurdles in radioimmunodiagnosis and radioimmunotherapy (*1*). Radioimmunoconjugates have been approved by the U.S. Food and Drug Administration for clinical oncology use (4 imaging agents, beginning with OncoScint [Cytogen Corp.] for imaging of tumor-associated glycoprotein 72 [TAG-72] in 1992 and Zevalin [Acrotech Biopharma] and Bexxar [GlaxoSmithKline] for therapy targeting CD20 in the early 2000s). However, clinical use (and hence, commercial success) has been hampered by unanticipated physician preferences (*2*) and numerous challenges universal to radiopharmaceutical therapies (*3*).

Despite the success in treating radiosensitive hematologic malignancies, radioimmunotherapy in the treatment of solid tumors has been clinically unsuccessful (*1*). Nevertheless, a recent revision of the radiobiologic paradigms of targeted α-therapy has revealed a highly complex response cascade comprising direct, bystander, and systemic effects (*4*), proving remarkably effective against β-refractive and bulky disease (*5*). Coupled with an enhanced development and application of theranostics in nuclear medicine, this response cascade has fueled development of a new generation of mAb theranostics against solid-tumor antigens, particularly with α-emitting

isotopes (e.g., City of Hope's anti–carcinoembryonic antigen [CEA] ^{225}Ac-DOTA-5MA NCT05204147; Bayer's suite of ^{227}Th-IgG drugs targeting mesothelin, prostate-specific membrane antigen, or human epidermal growth factor receptor 2 [HER2] antigens NCT03507452, NCT03724747, and NCT04147819; Janssen's ^{225}Ac-DOTA-h11B6 targeting human kallikrein 2 NCT04644770; and Fusion's ^{225}Ac-FPI-1434 targeting insulinlike growth factor type 1 receptor). More details can be found in several excellent reviews (*6–9*).

The field waits with great interest to see the outcome of these radioimmunotherapy clinical trials of directly labeled mAbs. Nonetheless, based on prior experience with other radioimmunotherapeutics, there is concern that hematopoietic toxicity will prove to be dose-limiting, a common hurdle for molecularly targeted radiopharmaceuticals (*3,10*). Fundamentally, the necessary therapeutic indices (TIs, or tumor–to–normal-tissue absorbed dose ratios) for meaningful radioimmunotherapy of solid-tumor masses were not achieved, partly because of inadequate mAb uptake (subtherapeutic radiation dose for solid tumors), dose-limiting toxicities (DLTs) because of poor TIs (causing myelotoxicity and renal toxicity), and antidrug antibodies (ADAs) (*1*). The radiopharmacology of radioimmunoconjugates has so far permitted mostly suboptimal TIs, especially for critical radiosensitive tissues such as bone marrow and kidney. Current and future advances in protein engineering and radioligand chemistry are necessary to overcome these barriers.

Pretargeted radioimmunodiagnosis (PRID) and pretargeted radioimmunotherapy (PRIT) separate the tumor targeting and the radiocarrier (e.g., a radiohapten) delivery steps, vastly improving the contrast and TIs while creating modular systems with individual optimization ease (Fig. 1). The tumor-targeting bispecific protein can be engineered to improve tumor uptake and TI; a chase molecule or clearing agent (CA) can be designed to sequester unbound proteins from blood to liver for metabolism. After an optimal pretargeting interval of hours or days, an intravenous payload with high affinity for the second specificity in the protein seeks out the bispecific protein targeted to the tumor or clears from the body in minutes to hours.

Current PRID and PRIT approaches harness advances in protein engineering and bioorthogonal chemistry to overcome the limitations of previous PRID and PRIT systems. However, PRID and PRIT present additional complexity in terms of drug manufacture (developing at least 2 products, and perhaps a CA) and dosing protocol optimization (both dose and pretargeting interval). Here, we provide a historical perspective of PRID and PRIT and explore potential ways by which PRID and PRIT can be further optimized to deliver a high radiation dose to tumor while improving TIs substantially for critical radiosensitive tissues.

HISTORICAL PERSPECTIVE

Concept of PRID and PRIT

Building on initial investigations of in vivo tumor targeting with radiolabeled polyclonal antibodies (*11,12*) and fueled by the discovery of mAbs by Köhler and Milstein (*13*), radioimmunodiagnosis using mAbs surged in the late 1970s, and radioimmunotherapy soon followed (*14,15*). However, despite the antigen specificity of mAbs, most did not translate into high-contrast tumor imaging (*15*). The critical hurdle—that is, disappointingly low overall tumor uptake and high normal-tissue background with radiolabeled IgG mAbs—was realized early on, requiring ^{99m}Tc blood-pool agents for computer subtraction from ^{131}I-mAb images (*16*).

In the mid 1980s, Goodwin et al. pioneered one of the first examples of pretargeting of radioisotopes by engineering metal chelate–specific mAbs (*17*). This example was predicated on the physicochemical properties of metal chelate complexes (often low-molecular-weight and hydrophilic combined with net negative charge and high kinetic stability under physiologic conditions) possessing extremely favorable in vivo pharmacokinetics and biodistribution. The antichelate mAb CHA255 passively entered tumors and, after a pretargeting interval of 24 h, was chased with a metal chelate hapten, indium (III)-4-[*N*′-(2-hydroxyethyl)thioureido]-L-benzyl-ethylenediaminetetraacetic acid (*18*). The concept of chelate chase—that is, using pharmacologic doses of an empty nonradioactive chelate hapten to force rapid renal excretion—significantly enhanced contrast, thereby reducing normal-organ radiation exposure by as much as 95% (*18,19*). Soon after, Stickney et al. conducted the first clinical trial of PRID in patients with CEA-expressing colorectal cancer (CRC) using a bispecific antibody (BsAb) anti-CEA/anti–metal chelate hapten system (*20*). Besides establishing the feasibility of the approach in this study of 14 patients, 20 of 21 known lesions were detected, for an overall sensitivity of 95%; 8 of 9 new lesions were confirmed; and high contrast was observed at as early as 4 h (Fig. 2A) (*20*).

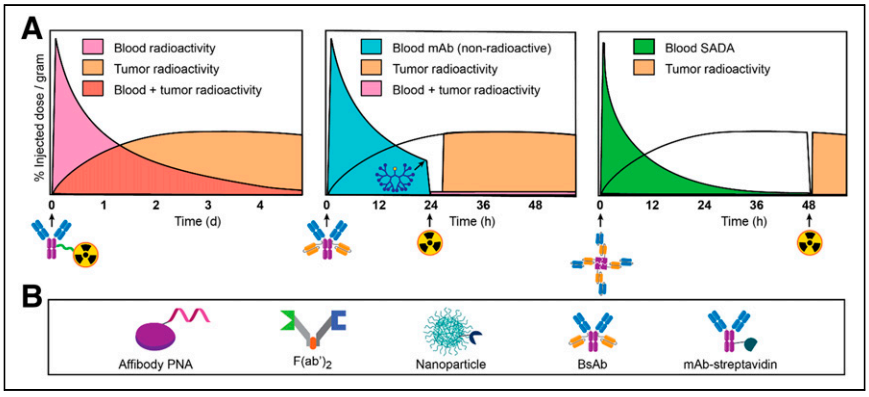

FIGURE 1. Comparison of conventional radioimmunotherapy and PRID/PRIT and compatible vector survey. (A) Injection of radioimmunoconjugate (left) leads to low TIs, especially in hematopoietic and highly perfused tissues. With 3-step BsAb pretargeting (middle), BsAb is administered, followed 1 d later by CA to quickly reduce circulating BsAb. During final step, administered radiocarrier (e.g., radiohapten) is captured by intratumoral BsAb or rapidly cleared. A 2-step approach (right) is feasible with SADA BsAb innovation. (Adapted from (*153*)). (B) Select bispecific antitumor/antiradiocarrier vectors.

A Surge in PRID—Especially Driven by Biotin–Streptavidin Approaches—and the Potential of PRIT

Although PRID with BsAb showed considerable promise, issues related to TIs as a consequence of insufficient affinity or avidity for the hapten (e.g., low-nanomolar range) prompted the development of alternatives. Streptavidin (53 kDa protein from the bacterium *Streptomyces avidinii*) and avidin (66 kDa protein found in egg whites) are both tetrameric proteins, with each individual subunit able to bind a single molecule of biotin (244 Da) with similar affinities (femtomolar). With these significantly higher affinities, the biotin–streptavidin system was an attractive candidate for pretargeting.

One of the first pretargeting applications of the biotin–streptavidin system was devised by Hnatowich et al. in 1987, consisting of an

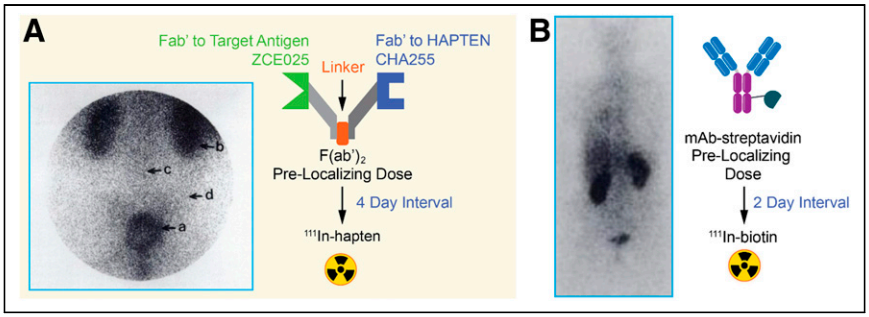

FIGURE 2. Initial PRID studies of tumors in patients. (A) BsAb pretargeting system. Planar posterior pelvic scan (coronal view) of patient with recurrent CRC invading right sacral area was obtained 3 d after injection of ^{111}In-hapten. a = tumor; b = kidneys; c = spine; d = iliac crest. (Reprinted with permission of (*20*).) (B) Biotin–streptavidin pretargeting system. Anterior chest and upper abdomen image (coronal view) of patient with recurrent squamous cell carcinoma of right lung was obtained 2 h after injection of ^{111}In-biotin. a = tumor; b = kidneys; c = bladder. (Reprinted from (*26*).)

antitumor mAb–streptavidin conjugate, a chase molecule, and radiolabeled biotin (*21*). Afterward (1987–1988), multiple research groups explored various biotin–streptavidin reagents, establishing the immunoreactivity and in vivo fate of biotinylated or mAb–streptavidin pharmacokinetics, clearance of radiolabeled forms of biotin and streptavidin, and safety in animals (*22,23*). Notably, Pimm et al. documented that radioiodinated avidin and streptavidin were cleared from the circulation via the kidneys, but with prolonged renal retention (*22*). In addition to issues of immunogenicity, this renal retention of streptavidin (and hence low TI for the kidney) became problematic and dose-limiting, prompting efforts at alleviation via chemical modification (e.g., with succinic anhydride or 1,2-cyclohexanedione) or engineering of recombinant streptavidin (*24,25*). In 1990, Kalofonos et al. reported the clinical feasibility of biotin–streptavidin PRID (*26*). In 10 patients with squamous cell carcinoma of the lung, the investigators infused antihuman milk fat globule antigen 1 mAb–streptavidin for tumor targeting, followed 2–3 d later with ^{111}In-biotin (*26*). Positive imaging was observed in 8 of 10 lung tumors (Fig. 2B) (*26*).

In 1991, Paganelli et al. conducted their first biotin–streptavidin PRID clinical study on 19 patients with a confirmed histologic diagnosis of tumors using an optimized 3-step regimen consisting of biotinylated anti-CEA mAb, an avidin chase, and ^{111}In-biotin (*27*). Tumors and metastases were detected in 18 of 19 patients (the remaining patient was a true-negative) less than 3 h after administration of ^{111}In-biotin by γ-scintigraphy, with no evidence of toxicity and with favorable contrast (*27*).

Although PRID showed promise, its development was soon blunted by the advent of oncologic ^{18}F-FDG PET/CT (*28*). Also, for diagnosis, sufficient image contrast and a single-day imaging procedure was achievable with rapidly clearing antibody-based probes. Unlike radioimmunodiagnosis, for which high tumor–to–normal-tissue contrast is necessary at only 1 specific time point, radioimmunotherapy requires high contrast at all time points in order to achieve high TIs. PRIT soon became the major platform to further the science and its clinical translation. The primary consideration for PRID is its theranostic potential: directing the surgical procedure to sites of the body with a high likelihood of finding antigen-bearing tumor, and performing dosimetry using quantifiable radioisotopes, a critical predictor of tumor response to PRIT. Tables 1 and 2 summarize the clinical and preclinical PRIT studies, respectively, with an emphasis on dosimetry and TIs described here.

Published in 1997, pilot clinical PRIT studies by Paganelli et al., using ^{111}In/^{90}Y-biotin targeting against various tumor types with anti-CEA, anti-TAG-72, and antitenascin mAbs (*29*), demonstrated that favorable TIs could be achieved. Mean absorbed doses (as cGy/37 MBq) to tumor, marrow, kidney, and liver were 15.2 ± 8.7, 1.1 ± 0.6 (TI, 13.8), 4.5 ± 2.1 (TI, 3.4), and 1.5 ± 1.0 (TI, 10.1), respectively. Eleven patients with various tumors (breast, brain, colon) were administered ^{90}Y-biotin doses ranging from 1.85 to 5.55 GBq; the treatment was well tolerated, and no acute toxicity was observed. However, ADA to streptavidin was observed in all patients.

Over the next decade, Paganelli et al. studied multiple biotin–streptavidin PRIT dosing protocols and injection routes (reviewed by Papi et al. (*30*)). Remarkably, from 1994 to 2005, over 500 glioblastoma patients were treated with biotin–streptavidin PRIT. For example, during a phase I/II study (*31*), they treated 48 patients (possessing histologically confirmed grade III and IV gliomas) using 5-step intravenous antitenascin PRIT with ^{111}In/^{90}Y-biotin (^{90}Y-biotin dose range, 2.22–2.96 GBq/m^2). The DLT was hematologic, and the maximum tolerated dose (MTD) was 2.96 GBq/m^2. They reported tumor, brain, kidney, liver, and marrow mean absorbed doses (as cGy/37 MBq) of 15.20 ± 8.70, 0.6 ± 0.3 (TI, 25.3), 2.7 ± 1.6 (TI, 5.63), 1.5 ± 1.0 (TI, 10.1), and 0.8 ± 0.5 (TI, 19.0), respectively. ADA to streptavidin was observed in all patients.

These early clinical PRIT studies inspired many groups to explore biotin–streptavidin PRIT in the mid to late 1990s (*32,33*). Much effort was devoted to improving BsAb design and alternative second specificities (besides biotin or metal chelator haptens), including complementary oligomeric pretargeting systems (*34–36*). Using morpholino complementary oligomers, Liu et al. and Hnatowich et al. have shown success for in vivo applications (reviewed by Liu (*37*)), although they have not been investigated clinically.

NeoRx Corporation exploited mAb–streptavidin fusion proteins to pretarget tumors before administration of radiobiotin. During the early to mid 1990s, they developed a mAb–streptavidin chemical conjugate (mAb NR-LU-10 specific for epithelial cell adhesion molecule) to target multiple solid-tumor types (*38*). In 2000, they showed how a single treatment with pretargeted ^{90}Y-biotin was curative in nude mice bearing human tumor xenografts (CRC, lung, and breast) without significant toxicity (*39*). Although TIs were not reported, an approximately 20-fold improvement in the tumor-to-blood area under the curve (AUC) ratio (calculated from 0 to 120 h after injection) for PRIT versus conventional radioimmunotherapy was demonstrated (tumor-to-blood AUC ratio: 28.3 and 1.22, respectively). At doses of up to 29.6 MBq (MTD not reached) of pretargeted ^{90}Y-biotin per mouse, 28 of 30 cures were achieved with transient myelosuppression and no apparent sequelae. Moreover, kidney uptake and retention were relatively low, at approximately 2% of the injected dose per gram from 2 to 120 h after injection. During a phase I dose escalation study (*40*), the MTD was determined to be 4.07 GBq/m^2, the DLT at 5.18 GBq/m^2 was gastrointestinal toxicity, and the recommended phase 2 dose was 4.44 GBq/m^2. These findings were considered highly remarkable because DLT was not hematologic and ^{90}Y doses approximately 5 times higher than radioimmunotherapy could be administered without marrow DLT or use of stem cell support (*41*). Imaging and dosimetry studies (*42*) revealed tumor, small-intestine, large-intestine, kidney, liver, and marrow mean absorbed doses

TABLE 1
Select Clinical PRIT and Targeted Radiotherapy Studies with Emphasis on Dosimetry

Year	Vehicle	TRT type	No. of steps	Antigen targets	Tumor types	No. of patients	RIT/PRIT radiocarrier	Administered activity	cGy/37 MBq to tumor	TI			Reference
										Marrow	Kidney	Liver	
1997	IgG–biotin	PRIT	5*	CEA, TAG-72, tenascin	Advanced metastatic (breast, brain, colon)	11	^{90}Y-biotin	1.85–5.55 GBq	15.2 ± 8.7	13.8	3.4	10.1	(*29*)
1997	IgG	RIT	1	TAG-72	Metastatic gastrointestinal tract carcinomas	12	^{90}Y-IgG	0.640–1.421 GBq	34.5 ± 24.6 (7.0–80.9)	15.2 (3.6–42.1)	ND	0.9 (0.3–1.5)	(*45*)
1998	mAb–streptavidin	PRIT	3	Epcam	Various†	40	^{90}Y-biotin	2.035–10.693 GBq (0.925–5.18 GBq/m^2)	16.4 ± 13.2	48.2	1.43	5.47	(*40,42*)
1999	IgG–biotin	PRIT	5*	Tenascin	High-grade glioma	48	^{90}Y-biotin	2.22–2.96 GBq/m^2	15.20 ± 8.70	19.0	5.63	10.1	(*31*)
1999	F(ab)′ × F(ab)′	PRIT	2	CEA	MTC	26	^{131}I-diDTPA(indium)-hapten	0.888–2.22 GBq/m^2 (1.41–4.14 GBq)	44.33 ± 53.39 (2.91–184)	29.62 ± 35.32	8.36 ± 10.02	10.86 ± 13.55	(*71*)
2000	mAb–streptavidin	PRIT	3	CD20	Non-Hodgkin lymphoma	7	^{90}Y-biotin	1.11 or 1.85 GBq/m^2	29 ± 23	181	5.8	18	(*41*)
2004	$(scFv)_4$–streptavidin	PRIT	3	CD20	Non-Hodgkin lymphoma	15	^{90}Y-biotin	0.555 GBq/m^2	26 ± 4 (2–69)	104	3.4	22	(*57*)
2005	$(scFv)_4$–streptavidin	PRIT	3	TAG-72	Metastatic CRC	9	^{90}Y-biotin	0.37 GBq/m^2	28.9 (4.18–121.6)	117.4 (25.8–399.1)	4.12	8.0 (1.9–17.6)	(*46*)
2014	DNL	PRIT	2	CEA	Metastatic CRC	20	^{177}Lu-IMP288	2.5–7.4 GBq	ND‡	^{177}Lu: 4.68 (0.68–10.91); simulated ^{90}Y: 5.41 (0.99–13.72)	ND	ND	(*110*)

*IgG-biotin/avidin chase/streptavidin/biotinylated albumin CA/^{90}Y-biotin.

†Refractory epithelial (including ovary, colon, prostate, breast).

‡Not reported as cGy/37 MBq, but based on absorbed doses to tumor determined using Monte Carlo-based 3D-RD dosimetry package (0.46–4.52 Gy) and corresponding administered activities (5.6 and 2.5 GBq for 0.46 and 4.52 Gy, respectively), range of 0.30–6.69 cGy/37 MBq was calculated.

TRT = targeted radiotherapy; RIT = radioimmunotherapy; ND = not determined.

All treatments were administered intravenously.

TABLE 2
Select Preclinical PRIT and Targeted Radiotherapy Studies with Emphasis on Dosimetry

Vehicle	TRT type	RIT/PRIT radiocarrier	cGy/MBq to tumor	cGy/37 MBq to tumor	TI			Reference
					Blood	Kidney	Liver	
IgG	RIT	^{131}I-3F8 (^{131}I-naxitamab)	237.4 ± 40.4	8,784 ± 1,495	3	13	19	(*51*)
F(ab′)$_2$	RIT	^{131}I-F6 F(ab′)$_2$	184	6,800	5	10	17	(*157*)
Peptide	PRRT	^{177}Lu-DOTATATE (Lutathera*)	34 ± 0.4	1,258 ± 14.8	ND	3	46	(*158*)
IgG–streptavidin	PRIT	^{177}Lu-biotin or ^{90}Y-biotin	^{177}Lu: 62	^{177}Lu: 2,294	^{177}Lu: 9	^{177}Lu: 2	^{177}Lu: 9	(*103*)
			^{90}Y: 134	^{90}Y: 4,958	^{90}Y: 12	^{90}Y: 4	^{90}Y: 8	
scFv–streptavidin	PRIT	^{90}Y-biotin	153.1 ± 8.3	5,665 ± 307	170	3	21	(*51*)
Antitumor F(ab′)$_2$ × anti-HSG Fab	PRIT	^{177}Lu-IMP241 or ^{90}Y-IMP241	^{177}Lu: 151	^{177}Lu: 5,587	^{177}Lu: 45	^{177}Lu: 9	^{177}Lu: 35	(*84*)
			^{90}Y: 388	^{90}Y: 14,356	^{90}Y: 35	^{90}Y: 8	^{90}Y: 26	
DNL	PRIT	^{177}Lu-IMP325 or ^{90}Y-IMP325	^{177}Lu: 72.8	^{177}Lu: 2,695	^{177}Lu: 169	^{177}Lu: 7	ND	(*91*)
			^{90}Y: 135	^{90}Y: 5,011	^{90}Y: 158	^{90}Y: 7		
IEDDA click	PRIT	^{177}Lu-Tz	556	20,572	11	21	26	(*140*)
DOTA-PRIT	PRIT	^{177}Lu-DOTA	85	3,145	142	23	40	(*120*)
Affibody-PNA	PRIT	^{177}Lu-HP2	108	3,996	269	5	81	(*132*)
SADA-PRIT	PRIT	^{177}Lu-DOTA	320	11,840	109	25	32	(*127*)

*Advanced Accelerator Applications.
TRT = targeted radiotherapy; RIT = radioimmunotherapy; ND = not determined; IEDDA = inverse electron-demand Diels–Alder.
All therapies were given intravenously to immunocompromised mice bearing subcutaneous human cancer xenografts.

(as cGy/37 MBq) of 16.4 ± 13.2, 49.2 ± 25.3 (TI, 0.33), 34.8 ± 17.9 (TI, 0.47), 11.5 ± 5.6 (TI, 1.43), 3.0 ± 1.8 (TI, 5.47), and 0.34 ± 0.08 (TI, 48.2), respectively. High doses of ^{90}Y-biotin in the gastrointestinal tract resulted from cross-reactivity of the mAb NR-LU-10 with the bowel epithelium. Moreover, tumor response was seen in the 2 patients with the highest estimated dose to tumor (4,000–6,000 cGy); grade IV diarrhea was observed in patients estimated to have received 6,850–14,000 cGy to the large-intestine wall; and delayed renal toxicity was observed in patients estimated to have received 2,170 or 3,072 cGy. In the same year, Knox et al. reported disappointing results from a phase II clinical study on 25 patients with metastatic CRC after a single dose of mAb–streptavidin pretargeted ^{90}Y-biotin, 4.07 GBq/m^2 (mean administered dose, 3.941 ± 0.381 GBq/m^2) (*43*). The overall response rate was modest (8%), and both hematologic and nonhematologic toxicities were observed (severe diarrhea in 30% of patients and delayed renal toxicity in 2 patients).

NeoRx moved on to an alternative pan-carcinoma mAb/antigen system, in which a mAb–streptavidin chemical conjugate (mAb CC49 specific for TAG-72) was used to deliver radiobiotin (*44*). Anti-TAG-72 radioimmunotherapy was studied clinically in the mid 1990s; for example, ^{111}In/^{90}Y-CC49 was evaluated in 12 patients with metastatic gastrointestinal tract carcinomas (*45*). Preclinical pretargeting studies on nude mice bearing human tumor xenografts were promising, as the tumor-to-blood AUC ratios were 179, 170, and 371 for ^{149}Pm-, ^{166}Ho-, and ^{177}Lu-biotin, respectively (no TIs were reported), and kidney uptake was minimal, at approximately 1%–2% of the injected dose per gram from 1 to 168 h after injection (*44*). In 2005, a phase I 3-step PRIT trial was performed using a CC49-(single-chain variable fragment [scFv])$_4$–streptavidin fusion (*46*). A total of 9 advanced-CRC patients received CC49-(scFv)$_4$–streptavidin, CA, and ^{111}In/^{90}Y-biotin (^{90}Y-biotin dose of 0.37 GBq/m^2). Imaging and dosimetry studies revealed a patient-specific mean ^{90}Y radiation dose (as cGy/37 MBq) of 7.02 (range, 3.36–11.2) to kidneys, 3.75 (range, 0.63–6.89) to liver, 0.22 (range, 0.12–0.34) to marrow, and 28.9 (range, 4.18–121.6) to tumors, corresponding to TIs of 4.12, 7.71, and 131 for kidney, liver, and marrow, respectively (*46*). MTD, DLT, and recommended phase 2 dose were not defined; however, the low TI for kidney was projected to be dose-limiting. Förster et al. demonstrated that succinylation of the CC49-(scFv)$_4$–streptavidin construct could reduce kidney uptake (*47*), but this was never tested clinically.

Additional solid-tumor mAb/antigen systems studied by NeoRx for PRIT included Lewis Y antigen (with ^{213}Bi-biotin (*48*) or ^{90}Y-biotin (*49*)) and mesothelin (with ^{177}Lu-biotin or ^{90}Y-biotin (*50*)). Also, using a novel antidisialoganglioside (GD2)-(scFv)$_4$–streptavidin fusion protein, highly efficient GD2 targeting was demonstrated with ^{111}In-biotin in nude mice bearing human tumor xenografts (*51*). Tumor-absorbed radiation doses (as cGy/37 MBq) were 8,784 ± 1,495 and 5,665 ± 307 for conventional radioimmunotherapy and PRIT with ^{90}Y-biotin, respectively (*51*). For radioimmunotherapy, TIs of 3, 13, and 19 were determined for blood, kidney, and liver, respectively. In comparison, for PRIT with ^{90}Y-biotin, TI was improved for blood (TI, 170) but diminished for kidney (TI, 3) and similar for liver (TI, 21). Although highly promising in terms of reducing myelotoxicity, the poor TI for kidney limited its translational potential.

NeoRx also developed reagents for PRIT of hematologic cancers. In the mid 1990s, remarkably, anti-CD20 radioimmunotherapy was shown to be curative in patients with relapsed B-cell lymphomas; however, highly aggressive myeloablative treatments with bone marrow rescue were needed (*52*). In 2002, the results from the anti-

CD20 radioimmunotherapy phase 3 study of ^{90}Y-ibritumomab were reported, showing that treatment was well tolerated and superior to rituximab in terms of overall response rate and complete response rate (*53*). NeoRx collaborated with Press et al. at the Fred Hutchinson Cancer Research Center and the University of Washington to develop anti-CD20 biotin–streptavidin PRIT to improve the safety profile of anti-CD20 radioimmunotherapy (*54*). They prepared an anti-CD20–streptavidin chemical conjugate for PRIT with ^{90}Y-biotin and performed preclinical studies on nude mice bearing human Ramos xenografts, making direct comparisons with radioimmunotherapy (*54*). Although no TIs were reported, tumor-to-blood ratios at 24 h were markedly improved with PRIT (3 and 0.4 for PRIT and radioimmunotherapy, respectively). Notably, superior tumor uptake was also shown with PRIT, establishing the potential advantage of PRIT particularly for noninternalizing antibodies. A lethal dose of 14.8 MBq was reported for radioimmunotherapy, with all treated animals dying of marrow suppression and infection on day 10. In contrast, 9 of 9 mice receiving pretargeted ^{90}Y-biotin (29.6 MBq) achieved CRs by day 12, leading to 8 of 9 cures (no recurrences during observation period of >140 d) and minimal toxicity.

These highly promising preclinical PRIT studies led to a phase I/II study on non-Hodgkin lymphoma patients (*41*). Seven patients with relapsed or refractory non-Hodgkin lymphoma received ^{111}In/^{90}Y-biotin (^{90}Y-biotin dose of 1.11 or 1.85 GBq/m^2). Tumor, kidney, liver, and marrow mean absorbed doses (as cGy/37 MBq) were 29 ± 23, 5.0 ± 1.7 (TI, 5.8), 1.6 ± 0.5 (TI, 18), and 0.16 ± 0.1 (TI, 181), respectively; also, the estimate of tumor–to–whole-body dose ratio (38:1) achieved with PRIT was higher than has been achieved using conventional radioimmunotherapy. Furthermore, doses of ^{90}Y 3 times the MTD of radioimmunotherapy could be given without significant myelosuppression. As a result, 6 of 7 achieved objective tumor regression, including 3 complete response and 1 partial response (*41*). Only grade I/II nonhematologic toxicity was observed, and grade III hematologic toxicity was transient in 5 of 7 patients. Six of 10 patients developed measurable ADA. MTD was not defined but was noted to be "likely more than 1.85 GBq/m^2" on the basis of dose-limiting hematologic toxicity, and kidneys showed the highest uptake (5.0 ± 1.7 cGy/37 MBq vs. 1.3 cGy/37 MBq for unbound radiobiotin (*55*)).

To generate well-defined and homogeneous fusion proteins and greatly simplify manufacturing, the group developed a second-generation, genetically engineered anti-CD20–streptavidin fusion protein (as a $(scFv)_4$–streptavidin fusion, B9E9FP (*56*)), documented a tumor-to-blood AUC ratio of more than 60 in nude mice bearing Ramos xenografts, and performed a phase I pilot trial in B-cell non-Hodgkin lymphoma (*57*). Fifteen non-Hodgkin lymphoma patients received B9E9FP, CA, and ^{111}In/^{90}Y-biotin (^{90}Y-biotin dose, 0.555 GBq/m^2). Mean absorbed doses to tumor, kidney, liver, and marrow (as cGy/37 MBq) were 26 ± 4, 7.7 ± 1.7 (TI, 3.4), 1.2 ± 0.2 (TI, 22), and 0.25 ± 0.04 (TI, 104), respectively. MTD, DLT, and recommended phase 2 dose were not defined. ADA was substantial 3 patients, and 5 patients had transient low antibody responses.

Additional hematologic tumor mAb/antigen systems studied by NeoRx for PRIT included CD25 (with ^{90}Y-biotin or ^{213}Bi-biotin (*58*)) and CD45 (with ^{90}Y-biotin (*59*)). In a notable study, Pantelias et al. (*60*) evaluated multiantigen PRID with mAb–streptavidin (anti-CD20, anti-human leukocyte antigen DR, anti-CD22) and ^{111}In-biotin. Interestingly, the most favorable tumor–to–normal-organ ratios of absorbed radioactivity were obtained using single conjugates optimized for target tumor antigen expression rather than the combination therapy (*60*). Of these additional PRIT systems, CD45 has been evaluated clinically.

Second-Generation BsAb PRIT with Multivalent Haptens

Alongside biotin–streptavidin PRIT development in the late 1980s, groups were also looking to optimize contrast by improving hapten selectivity for intratumoral BsAb over circulating BsAb. In 1989, Le Doussal et al. (Immunotech) evaluated PRID with bivalent hapten tracers to image CEA-expressing CRC (*61*). Coined "affinity enhancement," they showed greater affinity to cell-bound than to unbound BsAb via cooperative cross-linking of intratumoral BsAb, resulting in additional tumor-absorbed dose (*61*). Also, a chase or CA was not required for high contrast, greatly simplifying the pretargeting regimen. Around the same time, Goodwin et al. reported a bivalent Janus hapten for pretargeting with their antichelate mAbs (*62*).

Between 1993 and 1998, Immunotech performed clinical PRID studies with an anti-CEA mAb/metal chelate–specific mAb BsAb. The metal chelate-specific mAb was against indium-diethylenetriaminepentaacetic acid (indium-DTPA). With a bivalent ^{111}In-diDPTA-tyrosyl-lysine hapten for PRID, they demonstrated that high-contrast images could be obtained in patients with CRC (*63*), medullary thyroid cancer (MTC) (*64,65*), and small-cell lung cancer (*66*). Although the images were impressive, the use of murine BsAb led to ADA in most patients (e.g., ~60% (*63*)). Furthermore, for PRIT with ^{131}I, instead of developing a new metal chelate–specific mAb, they used stable indium-DTPA as an affinity handle to generate ^{131}I-labeled diDTPA(In)-tyrosyl-lysine radiohapten (^{131}I-diDTPA(indium)-hapten) and analogs for chelation of ^{99m}Tc and ^{188}Re (*67–69*). In nude mice bearing human MTC xenografts, pretargeting of 92.5 MBq of ^{131}I-diDTPA(indium)-hapten was demonstrated to be more efficient (leading to significantly longer growth delays) and less toxic than radioimmunotherapy (*70*). Soon after, this approach was evaluated in patients.

Initially, 2 phase I/II clinical trials assessing PRIT with ^{131}I-diDTPA(indium)-hapten were performed on patients with either MTC (*71*) or small-cell lung cancer (*72*). The BsAb was a F(ab)′ × F(ab)′ chemical conjugate. Twenty-six MTC patients received 1–3 treatments at ^{131}I-diDTPA(indium)-hapten doses ranging from 0.888 to 2.22 GBq/m^2 (*71*). Tumor, kidney, liver, and marrow mean absorbed doses (as cGy/37 MBq) were 44.33 ± 53.39, 5.61 ± 2.02 (TI, 8.36 ± 10.02), 5.19 ± 2.23 (TI, 10.86 ± 13.55), and 1.60 ± 0.82 (TI, 29.62 ± 35.32), respectively (*71*). Myelosuppression was the crucial factor for DLT, and MTD (and recommended phase 2 dose) was 1.78 GBq/m^2 (*71*). Among the 17 evaluable patients, 5 minor tumor responses were observed in patients with mainly a small tumor burden (*71*). ADA was observed in 9 of 17 (53%) patients (*71*). During the second clinical trial, 14 patients with small-cell lung cancer were treated with ^{131}I-diDTPA(indium)-hapten ranging from 1.48 to 6.66 GBq (*72*). Tumor, kidney, liver, and marrow absorbed doses (as cGy/37 MBq) were 1.8–32.2, 3.9–5.0, 1.6–5.0, and 0.4–1.7, respectively. MTD without hematologic rescue was 5.55 GBq (*72*). Of the 12 patients, 2 partial response and 1 stabilization of more than 24 mo was observed (*72*). Although no recommended phase 2 dose was specified, dose escalation was reported to be continuing to reach 11.1 GBq (*72*). Among 5 evaluable patients for ADA, 1 patient showed significant ADA after 2 mo, which persisted at 12 mo (*72*).

A subsequent clinical trial was performed to optimize reagent dosing and timing of administration with humanized BsAb in 35 patients with CEA-expressing tumors (*73*). BsAb doses ranged from 10 to 100 mg/m^2, ^{131}I-diDTPA(indium)-hapten doses ranged from 1.9 to 5.5 GBq, and a pretargeting interval of 5 or 7 d was

studied (*73*). With optimized PRIT (e.g., with 40 mg/m^2 of BsAb and a 5-d pretargeting interval), ^{131}I-diDTPA(indium)-hapten doses of up to 5.5 GBq were well tolerated in the absence of bone marrow involvement (*73*).

In a follow-up trial on 22 patients with CEA-expressing tumors, the humanized BsAb dose (40–75 mg/m^2) and ^{131}I-diDTPA(indium)-hapten dose (1.8–2.9 GBq/m^2; 1.9–5.5 GBq) were varied to evaluate antitumor efficacy and toxicity (*74*). Myelosuppression was BsAb dose–dependent, with 75 mg/m^2 leading to high hematologic toxicity, and nonhematologic toxicity was hepatic (transient grade I or II) (*74*). With a BsAb dose of 75 mg/m^2, higher whole-body and liver mean radiation doses were observed (0.38 and 1.9 Gy for whole body and liver, respectively) than for 40 mg/m^2 (0.33 and 1.4 Gy for whole body and liver, respectively), and mean tumor doses did not differ significantly with BsAb dose (75 mg/m^2, 10.7 Gy [range, 1.7–53.5 Gy]; 40 mg/m^2, 18.5 Gy [range, 2.4–49.3 Gy]) (*74*). Modest therapeutic efficacy was reported, with no CRs or PRs (*74*). The MTD was determined to be 3 GBq of ^{131}I-diDTPA(indium)-hapten in MTC patients and was not defined in non-MTC patients (escalated beyond 5.5 GBq) (*74*). Human antimouse antibody elevation was observed in 1 patient (8%), and human antihuman antibody was observed in 4 patients (33%) (*74*).

In 2006, Chatal et al. reviewed their clinical experience and compared the survival of advanced-MTC patients who underwent PRIT (^{131}I-diDTPA(indium)-hapten doses ranging from 1.9 to 5.5 GBq) with that of contemporaneous untreated patients for whom data were collected by the French Endocrine Tumor Group (*75*). Notably, they showed a survival benefit for those treated with PRIT, underscoring its clinical promise (*75*).

Besides CEA-expressing tumors, a PRID approach to imaging renal cell carcinoma was developed with bivalent haptens. Use of an anti–renal cell carcinoma/anti–indium-DTPA hapten BsAb and a refined tetrapeptide bivalent hapten, ^{111}In-diDTPA-Phe-Lys-Tyr-Lys (^{111}In-diDTPA-FKYK), showed highly efficient tumor targeting (*76,77*). During comparative studies with monovalent ^{111}In-DTPA and ^{111}In-diDTPA-FKYK, they achieved dramatic improvements in tumor uptake with the bivalent hapten (in nude mice bearing human renal cell carcinoma xenografts: ~78% vs. ~2% of the injected dose per gram at 4 h after injection for the bivalent and monovalent haptens, respectively) without sacrificing promising tumor-to-blood ratios (*76*). The ^{111}In-diDTPA-FKYK was also prepared with D-amino acids to make it more resistant to in vivo peptidases and improve the residualization of ^{125}I during PRIT (*78*). Efficient targeting of CEA was also demonstrated via this approach (with ^{111}In, ^{99m}Tc, nonresidualizing ^{125}I, or residualizing ^{125}I) (*79*); however, antichelate mAbs were falling out of favor compared with alternative antihapten mAbs.

Third-Generation BsAb PRIT with Anti–Histidine-Succinyl-Glycine (HSG) mAb and BsAb Prepared via Dock-and-Lock (DNL)

The anti–^{111}In-DTPA hapten approach was limited by mAb specificity and could not be used to target ^{90}Y or ^{177}Lu (*80*). Although additional antichelate mAbs were prepared (e.g., anti–copper-triethylenetetramine and anti–yttrium-1,4,7,10-tetraazacyclododecane-1,4,7,10-tetraacetic acid (yttrium-DOTA) (*81*)), alternative antihapten mAbs were evaluated for PRIT, including anti-2,4-dinitrophenyl (*61*) and anti-HSG pseudopeptide (*82*). Also, around this time, novel BsAb formats with divalent tumor-antigen binding (e.g., anti-CEA IgG or anti-CEA F(ab′)$_2$ chemically conjugated to anti–indium-DTPA Fab′) were studied (*83*). Notably, pretargeting with anti-CEA IgG × anti–indium-DTPA Fab′ led to the most favorable tumor uptake and retention in the tumor, but use of a CA was necessary to achieve acceptable tumor-to-blood ratios (*83*). Therefore, a F(ab′)$_2$–Fab′ BsAb (~80 kDa) was considered optimum in terms of balancing tumor uptake and clearance without the need for a CA step (*83*).

In 2003, Sharkey et al. significantly advanced the HSG system for PRIT by developing a novel BsAb (e.g., anti-CEA F(ab′)$_2$ or anticolon-specific antigen-p F(ab′)$_2$ chemically conjugated to anti-HSG Fab) and a suite of HSG peptides suitable for targeting a variety of clinically relevant radionuclides (IMP241 for ^{90}Y, ^{111}In, and ^{177}Lu, and IMP245 for ^{99m}Tc and ^{188}Re) (*84*). Dosimetry projections for pretargeting anticolon-specific antigen-p with ^{90}Y- or ^{177}Lu-IMP241 in nude mice bearing human xenografts were 5,587–14,356 cGy/37 MBq for tumor, with corresponding TIs of 35–45, 8–9, and 26–35 for blood, kidney, and liver, respectively (*84*). In 2005, they clearly demonstrated the advantage of this pretargeting approach over a clinically used ^{99m}Tc-labeled CEA-specific F(ab′) for CRC imaging in mice bearing human xenografts (*85*). In 2006, an alternative peptide scaffold to IMP241 with less kidney retention was developed. IMP288 and PRID with ^{124}I was reported (*86*).

As was done for mAb–streptavidin fusions for biotin–streptavidin pretargeting, recombinant antitumor/antihapten BsAbs were replacing chemical conjugates. In 2003, Rossi et al. described a trivalent BsAb (hBS14: bivalent CEA and monovalent HSG); however, the engineering approach using transgenic myeloma cells led to low expression yield (*87*). Soon after, they described the DNL approach to assemble a multivalent tri-Fab antitumor/anti-HSG hapten BsAb with a molecular weight of approximately 157 kDa by exploiting regulatory protein kinase A dimerization and docking domains, and the anchoring domain of an interactive A-kinase anchoring protein, to form a stably tethered complex (Fig. 3A) (*88,89*). Interestingly, the blood clearance of the DNL BsAb was much faster than that of IgG (~150 kDa) since the BsAb lacks the CH_2 domain to enable neonatal Fc receptor recycling. DNL BsAbs have been generated against a variety of tumor antigens, including CEA (TF2), CD20 (TF4), and trophoblast cell surface antigen 2 (TF12); detailed reviews have been published (*28,90*). Dosimetry results for IMP325 (i.e., IMP288 saturated with nonradioactive indium) pretargeted to CEA-expressing LS-174T human CRC subcutaneous tumors were quite favorable; for example, for pretargeting of ^{177}Lu-IMP325, the authors reported TIs of 169 and 7 for blood and kidney, respectively, with an estimated tumor-absorbed dose of 2,695 cGy/37 MBq (*91*).

In one notable DNL PRIT preclinical study, they prepared anti-PAM4-antigen BsAb TF10 for targeting of ^{90}Y-IMP288 (*92*). They demonstrated in nude mice bearing established Capan-1 human pancreatic cancer xenografts that PRIT could be safely combined with gemcitabine and CRs could be achieved (*92*). Furthermore, they showed that doses of up to 33.3 MBq of pretargeted ^{90}Y-IMP288 were well tolerated over 9 mo with no evidence of chronic nephrotoxicity (MTD not reached), a marked improvement from initial ^{90}Y-IMP288 PRIT studies (*93*).

Initial clinical experience with the DNL BsAb platform included a phase 0 clinical study of ^{131}I-TF2 in 2 patients with suspected CRCs to characterize the clearance kinetics of the BsAb, and a first-in-patients PRID study with ^{111}In-IMP288 in a metastatic CRC patient (*94*). Although optimization of the TF2 dose was necessary, highly promising dosimetry projections of PRIT with ^{90}Y-IMP288 were reported (kidney, 1.4 cGy/37 MBq; marrow, 0.1 cGy/37 MBq) (*94*). Soon afterward, PRIT clinical trials with ^{111}In/^{177}Lu-IMP288 commenced.

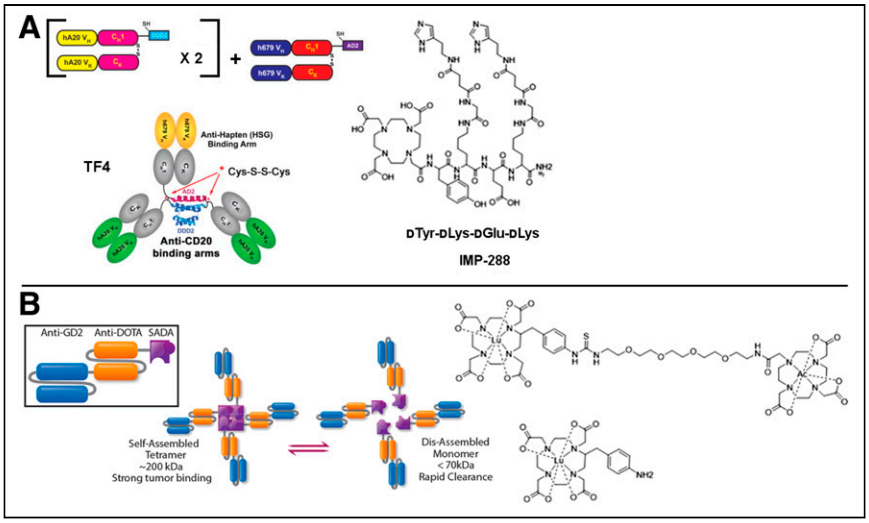

FIGURE 3. BsAb pretargeting with DNL BsAb or with SADA BsAb platform. (A) Structure of tri-Fab TF4 made by DNL method and associated HSG hapten, IMP-288. DNL BsAb has single binding site for hapten and 2 binding sites for tumor antigen. (Reprinted with permission of (*154*).) (B) Structure of anti-GD2/anti-DOTA SADA BsAb and ^{225}Ac-DOTA-hapten (reprinted from (*123*)) and ^{177}Lu-aminobenzyl-DOTA (reprinted with permission of (*127*)). SADA BsAb has 4 binding sites for both DOTA hapten and tumor antigen. hA20 = humanized anti-CD20 IgG hA20 (veltuzumab); VH = heavy chain variable domain; VK = light chain variable domain; CH1 = heavy-chain constant domain 1; CK = light-chain constant domain; DDD2 = dimerization and docking domain with SEQ ID NO: 2; AD2 = anchoring domain with SEQ ID NO: 4.

SELECTED PRETARGETING ADVANCES OF THE PAST DECADE

PRIT with Biotin–Streptavidin System

In 2013, Mawad et al. reported clinical PRIT with ^{111}In/^{90}Y-biotin in high-risk acute myeloid leukemia/myelodysplastic syndrome patients undergoing allogenic hematopoietic cell transplantation (*95*). Five patients received a 0.7 mg/kg dose of anti-CD45 mAb–streptavidin followed 48 h later by a 1.3 mg/m^2 dose of ^{90}Y-biotin (median, 2.775 GBq; range, 2.294–4.144 GBq) based on ^{111}In-biotin pretreatment dosimetry (*95*). No participants were withdrawn from the study because of toxicities; 2 grade 3 gastrointestinal adverse events (enterocolitis, typhlitis) were identified as unexpected and considered possibly related to PRIT, with the only grade 4 event being expected hematopoietic cell transplantation–related cytopenia (*95*). A single patient was in complete remission a year after protocol treatment, and the other 4 patients died of progressive disease, with a median time to relapse of 28 d (range, 12–155 d) (*95*).

More recently, in 2015, a trial was initiated with anti-CD20 B9E9 with ^{111}In/^{90}Y-biotin in patients with high-risk B-cell malignancies to evaluate the safety of combining PRIT with carmustine, etoposide, cytarabine, and melphalan chemotherapy and autologous stem cell transplantation (NCT02483000).

Paganelli et al. performed a locoregional PRIT clinical trial on 11 breast cancer patients (*96*). Avidin was injected around the tumor, followed by intravenous administration of 111 MBq of ^{90}Y-biotin. Remarkably, ADA to avidin has been shown to not limit therapy (*97*). De Santis et al. described AvidinOX (Alfasigma S.p.A.), an avidin variant designed to prolong the tissue half-life (2 wk compared with 2 h for native avidin) and to demonstrate cellular and interstitial protein tropism for enhanced PRIT (*98*). In addition to showing therapeutic promise in preclinical studies (*98–101*), AvidinOX PRIT has been studied in clinical investigations (NCT02053324 and NCT03188328, both of which were terminated because of low recruitment).

Preclinically, PRIT development continued (e.g., with ^{211}At-biotin-succinylated poly-L-lysine (*102*), and comparative efficacy of ^{177}Lu and ^{90}Y for anti-CD20 PRIT of B-cell lymphomas (*103*)). However, a head-to-head study comparing the efficacy and toxicity of anti-CD20 biotin–streptavidin PRIT and a novel BsAb PRIT platform with an ultra-high-affinity anti-yttrium-DOTA scFv antibody (C825) revealed preferred use of BsAb PRIT in future clinical trials (*104,105*).

BsAb Pretargeting

The DNL system has been extensively studied both preclinically (primarily in the development of additional haptens) and clinically, with multiple trials featuring DNL anti-CEA TF2 and radiolabeled IMP288. Two notable hapten developments included a novel radiolabeled/near-infrared multimodal DNL hapten, RDC018, for image-guided surgery of various carcinomas (*106*) and ^{213}Bi-IMP288 for α-PRIT (*107*).

In 2013, a landmark phase I PRIT study was reported with ^{111}In/^{177}Lu-IMP288 in 20 patients with CEA-expressing CRC (*108*). The ^{177}Lu-IMP288 dose was designed to deliver no more than 1.25 Gy to marrow or 15 Gy to kidneys (3.7–7.4 GBq) based on pretreatment dosimetry with ^{111}In-IMP288. Absorbed doses were less than 1.85 cGy/37 MBq for kidney, and mean marrow dose ranged from 0.0296 to 0.222 cGy/37 MBq based on the dosing cohort (*109*). Tumor doses were 0.46–4.52 Gy, and red marrow doses ranged from 0.12 to 0.97 Gy (mean TI, 4.68) (*110*). Furthermore, they projected an approximately 25% higher marrow TI for treatment with ^{90}Y-IMP288 instead of ^{177}Lu-IMP288 (mean TI simulated for ^{90}Y-IMP288, 5.41). DLT was hematologic, and no recommended phase 2 dose was indicated. Since TF2 is humanized and lacked Fc, ADAs were unexpected but observed in about 50% of the patients on repeated injection. However, a reduced infusion rate and preadministration of prophylactics were effective at reducing associated adverse events. A PRIT trial with ^{90}Y-IMP288 in metastatic CRC patients is ongoing (NCT02300922).

Soon after the phase I PRIT study in CRC patients, a phase I PRIT study with ^{111}In/^{177}Lu-IMP288 on 9 patients with CEA-expressing small-cell lung cancer was reported in 2015 (*111*), and first-in-humans PRID with TF2/^{68}Ga-IMP288 in MTC patients was reported in 2016 (*112*). In the last 2 y, additional clinical studies with TF2/^{68}Ga-IMP288 were performed on CRC (*113*) and HER2-negative/CEA-positive metastatic breast cancer patients (*114*). In 2021, Bodet-Milin et al. reported clinical data using TF2/^{68}Ga-IMP288 in MTC patients, demonstrating improved sensitivity for metastatic lesion detection over ^{18}F-L-dihydroxyphenylalanine PET/CT (*115*). Select examples of recent clinical PRID studies with TF2/IMP288 are shown in Figure 4.

Alongside the DNL BsAb pretargeting system, 2 additional BsAb pretargeting approaches using ultra-high-affinity (picomolar to femtomolar) antichelate mAbs have made significant progress in the last decade. Orcutt et al. affinity-matured the anti-DOTA chelate mAb 2D12.5 (*62*) and reformatted it as an scFv called C825 (*116*). C825 was shown to bind DOTA complexes of lutetium, yttrium, and gadolinium with similar affinity (low-picomolar range) (*116*).

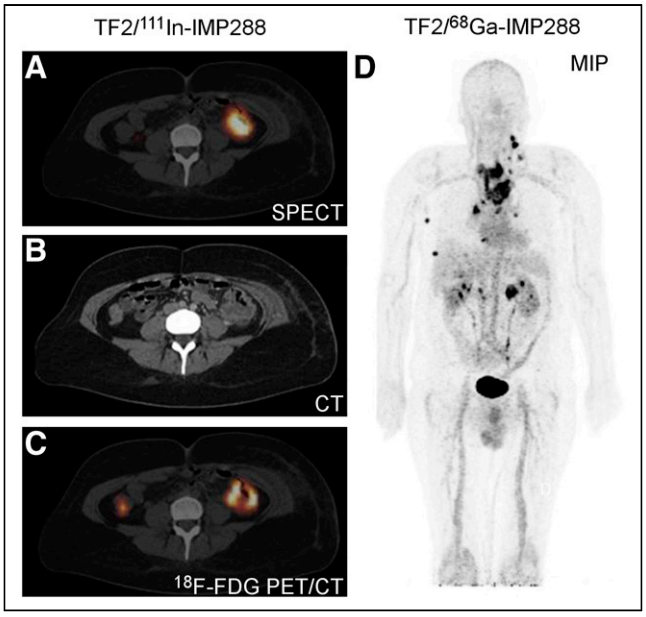

FIGURE 4. Select examples of recent clinical BsAb PRID with DNL TF2 and radiolabeled IMP288 (TF2/IMP288). (A) Scintigraphic images (axial views) of CRC patient imaged with TF2/^{111}In-IMP288, with highly specific targeting of primary colon tumor, confirmed by CT and ^{18}F-FDG PET/CT (B and C, respectively). (Reprinted from (*108*).) (D) PET image (coronal view) of MTC patient imaged with TF2/^{68}Ga-IMP288, with maximum-intensity-projection (MIP) image showing several pathologic lesions. (Reprinted from (*115*).)

Also, Orcutt reported a highly modular tetravalent IgG-scFv BsAb format (*117*) and carefully screened candidate DOTA-radiohaptens to determine which had the most favorable in vivo properties for PRIT, reporting estimated human liver, kidney, and red marrow doses for ^{90}Y-labeled haptens of 0.130–0.192, 0.703–0.999, and 0.029–0.048 cGy/37 MBq respectively (*118*). Also, in combination with a dextran-hapten CA, highly efficient anti-CEA mAb/C825 pretargeting with ^{177}Lu- or ^{111}In-haptens in nude mice bearing LS174T human CRC xenografts was demonstrated (*119*). These studies led to the antichelate BsAb platform called DOTA-based PRIT, or DOTA-PRIT. Between 2014 and 2018, Cheal et al. demonstrated DOTA-PRIT with ^{177}Lu-DOTA-hapten targeting a wide variety of solid tumors (antigen targets: GD2 (*120*), glycoprotein A33 (*121*), HER2 (*122*)). More recently, that team developed a ^{225}Ac-DOTA-hapten for α-PRIT (*123*). When DOTA-PRIT was used to pretarget ^{177}Lu-DOTA-hapten in nude mice bearing human xenografts, TIs of 28–142 for blood, 7–23 for kidney, and 12–47 for liver were achieved, with estimated tumor-absorbed doses ranging from 1,476 to 8,473 cGy/37 MBq (*120,122,124*). Notably, the lowest TIs (blood, 28; kidney, 7; and liver, 12) and estimated tumor dose (1,476 cGy/37 MBq) were observed for the anti-HER2 DOTA-PRIT system, which is known to internalize (*122*). Green et al. also used C825 BsAb for pretargeting ^{90}Y-DOTA-hapten to a variety of hematologic cancer targets (e.g., CD20 (*104*), CD45 (*125*), and CD38 (*126*)), reporting TIs of 6.75–21.4 for blood, 15.9–24.9 for kidney, and 5.52–7.24 for liver, with estimated tumor-absorbed dose ranging from 3,981 to 7,781 cGy/37 MBq.

Santich et al. reported a novel BsAb platform designed as a fusion of a self-assembling-and-disassembling (SADA) domain to a tandem single-chain BsAb for highly efficient 2-step radiohapten pretargeting (Fig. 3B) (*127*). With anti-GD2 SADA-PRIT plus ^{177}Lu-DOTA-hapten in nude mice bearing human cancer xenografts, an exceptional balance of high tumor targeting and high TIs was achieved: TIs were 100 for blood, 25 for kidney, and 32 for liver, with estimated tumor-absorbed dose of 11,840 cGy/37 MBq. Also, safe and tumoricidal anti-GD2 SADA-PRIT plus ^{177}Lu-DOTA-hapten or ^{225}Ac-DOTA-hapten was established (*127*). Initial clinical trials of anti-GD2 SADA-PRIT plus ^{177}Lu-DOTA-hapten are planned for this year on patients with recurrent or refractory metastatic GD2-expressing solid tumors, including small-cell lung cancer, sarcoma, and malignant melanoma (NCT05130255).

In 2018–2019, the team of Hoffmann-La Roche, Inc., and Orano Med LLC described a novel BsAb antitumor/antichelate hapten pretargeting system (antigen targets: CD20, HER2, and CEA) based on an anti-1,4,7,10-tetrakis(carbamoylmethyl)-1,4,7,10-tetraazacyclododecane (DOTAM) antibody with femtomolar affinity for lead-DOTAM complexes (*128*). Specifically, for the anti-CEA/DOTAM BsAb PRIT-0213, they reported dissociation constants of 0.84 pM and 5.7 pM for lead-DOTAM and bismuth-DOTAM, respectively (*128*). In nude mice bearing human cancer xenografts, they reported dosimetry for 3-step pretargeting (i.e., with CA) of 0.74 MBq of ^{212}Pb-DOTAM. On the basis of relative biologic effectiveness equal to 5, they estimated an absorbed dose of 99.55 Gy to BxPC3 tumor and TIs of 28, 14, and 91 for blood, kidney, and liver, respectively (*128*). Also, they highlighted preclinical anti-CEA PRIT therapy results, detailing strong tumor growth inhibition and significantly prolonged survival with 3 cycles of 1.11 MBq (*129*).

Harnessing Affibody (Affibody AB) Molecules as PRIT Vectors

Although IgG-based mAbs and BsAb have traditionally been used as PRIT vectors, their prolonged circulation can make timing of complete clearance difficult, leading to unintended bystander toxicity. Advances in protein engineering have given rise to alternative protein constructs such as minibodies (80 kDa), diabodies (50 kDa), and engineered scaffold proteins (4–20 kDa) (*6*). These smaller constructs have proven to be especially favorable as radionuclide imaging vectors (*6*). Affibody molecules are a highly promising class of engineered scaffold proteins that can be optimized to have high affinity and slow internalization kinetics. The anti-HER2 Affibody radiolabeled with ^{111}In (^{111}In-ABY-025) has been investigated clinically for imaging of disseminated HER2-expressing breast cancer (*130*). However, as vectors for radioimmunotherapy, Affibody molecules have been shown to be suboptimal for residualizing radiometal labels, leading to significant renal uptake (*131*).

Between 2016 and 2021, numerous studies describing Affibody PRID and PRIT were reported (*132,133*). Figure 5 illustrates and contrasts the pretargeting systems: first is an approach using synthetic DNA-analog peptide nucleic acids (PNAs) originally described by Hnatowich et al. in 1997 for PRID with ^{99m}Tc (*35*), and further work applying a bioorthogonal approach using click chemistry (described in the following section). A PNA strand is covalently conjugated to a targeting vector, in this case, an Affibody, and the radionuclide payload is delivered on a complementary PNA strand, injected after an optimized pretargeting interval of 16 h (*132*). The hybridization of complementary PNAs as a pretargeting technique supplies several advantages, including high affinity (picomolar dissociation constant), low immunogenicity, and resistance to in vivo degradation (*132*). For the Affibody-PNA approach, they reported for PRIT with ^{177}Lu-PNA (^{177}Lu-HP2) in nude mice bearing human cancer xenografts an estimated absorbed dose of 3,996 cGy/37 MBq to tumor and TIs of 269, 5, and 81 for blood, kidney, and liver, respectively (*132*). These results were

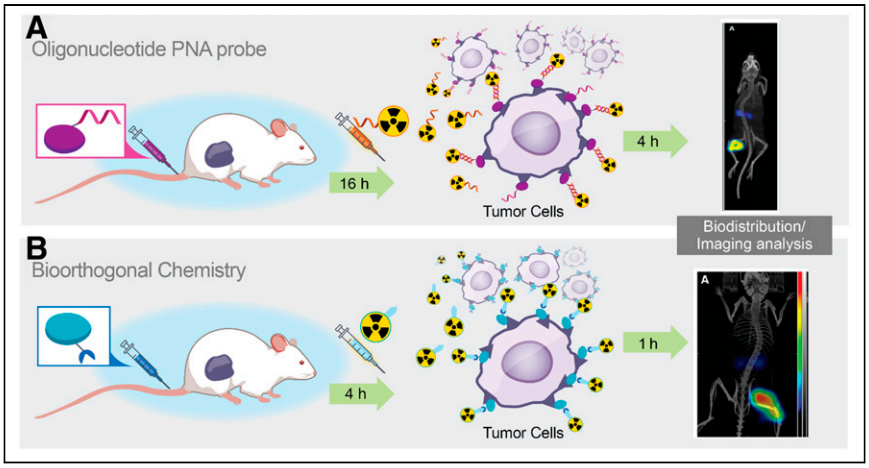

FIGURE 5. Affibody pretargeting with PNAs (A) or bioorthogonal inverse electron-demand Diels–Alder click chemistry (B). (Portions reprinted from (*133,155*).)

achieved using a 2-step approach, that is, without using CA. PRIT treatment efficacy was established using a fractionated PRIT approach (total administered ^{177}Lu-HP2, 96 MBq/mouse) in nude mice bearing subcutaneous SKOV-3 xenografts. Median survival was significantly prolonged in PRIT-treated mice in comparison to controls, and treatment was well tolerated, with no nephrotoxicity (*132*). Interestingly, they reported less efficient Affibody-PRIT using the bioorthogonal chemistry approach; although mouse dosimetry was not reported, the tumor-to-kidney AUC ratio was only 1.4 (*133*). However, this was a marked improvement from conventional Affibody-radioimmunotherapy, which results in a tumor-to-kidney AUC ratio of less than 1 and shows the promise of PRIT to substantially reduce radiometal accumulation in the kidneys with engineered scaffold proteins (*132*).

Bioorthogonal Pretargeting

Meares' elegant affinity capture pretargeting strategy, consisting of an antibody/ligand pair with complementary reactive groups that become covalently linked when they are near the antibody/ligand complex, was applied to antichelate mAb-based reporter gene imaging for noninvasive tracking of chimeric antigen receptor T cells by Krebs et al. (*134*). In contrast to affinity capture, with the very rapid kinetics of the bioorthogonal inverse electron-demand Diels–Alder click reaction ($k_2 > 10^3$ $M^{-1}s^{-1}$), probe attachment can occur by direct reaction with a chemically modified antibody (*135,136*). In 2010, initial in vivo PRID studies with the inverse electron-demand Diels–Alder reaction were reported (*137*). Soon after, many groups took an interest. Early development efforts included novel tetrazine-based radioprecursors for numerous radioisotopes, second-generation radiolabeled tetrazine molecules with improved pharmacokinetic and biodistribution properties, and incorporation of a chase step or CA (reviewed recently by Rondon and Degoul (*138*)).

Significant progress has also been made for PRIT using transcyclooctene-modified mAbs and radiolabeled tetrazine for inverse electron-demand Diels–Alder. In 2017, PRIT was demonstrated using ^{212}Pb-tetrazine in mice bearing TAG-72–expressing human CRC xenografts (*139*). Between 2017 and 2018, PRIT using ^{177}Lu-tetrazine (*140,141*) and ^{225}Ac-tetrazine (*142*), respectively, was demonstrated in multiple human tumor xenografts (CRC and pancreatic). For PRIT with ^{177}Lu-tetrazine in nude mice bearing human xenografts, TIs of blood (10.4–17.7), kidney (12.0–19.9), and liver (19.0–40.1) were achieved, with estimated tumor-absorbed doses ranging from 9,472 to 30,821 cGy/37 MBq (*140,143*). Moreover, PRIT with the highly promising ^{64}Cu/^{67}Cu pair was recently reported (*144*), with the authors nicely demonstrating efficient sequential radiolabeled tetrazine administration and safe and effective theranostic treatment. For PRIT with ^{67}Cu-tetrazine, the authors reported TIs of 6.5–9.7 for blood, 7.2–9.1 for kidney, and 4.0–4.2 for liver, with estimated tumor-absorbed doses ranging from 2,116 to 2,331 cGy/37 MBq depending on the pretargeting interval (*144*).

Recent efforts at bioorthogonal pretargeting development have focused on a combination of new chemistries (e.g., adamantane/cucurbituril (*145*)), new vectors (e.g., with nanoparticles (*146*); also, more details are provided in a recent review (*147*)), and continued optimization of radiolabeled tetrazine (*148*). Clinical bioorthogonal pretargeting chemotherapy trials are ongoing (NCT04106492), and bioorthogonal PRID trials are planned for the near future (*149*).

A ROAD MAP FOR DEVELOPMENT: RADIOBIOLOGIC GOALS OF PRIT

Our goal for PRIT should be to cure the tumor while safeguarding against excessive toxicity to normal tissues. To achieve this, we need better methods for dosimetry of internal radioemitters. We suggest that *Primer 2020,* the Medical Internal Radiation Dosimetry Committee publication soon to be released by the Society of Nuclear Medicine and Molecular Imaging, has provided us with the computational basis for tumor and normal-tissue dosimetry measurement to meet the goal of safe and efficacious targeted radiotherapy of advanced human tumors. Supplemental Figure 1 and the other supplemental information provide a more detailed rationale (supplemental materials are available at http://jnm.snmjournals.org).

As a starting point for radiation doses needed for curing while avoiding catastrophic damage to normal tissue, we propose the following. In a prior publication, we suggested quantitative radiobiologic targets to be met to achieve a high probability of cure for solid human tumors (*1*). The reasoning is that a sufficient radiation dose (cGy) must be absorbed by all cells in the tumor while minimizing the dose absorbed by normal tissues (i.e., the maximizing of TI). A series of reasonable benchmarks for effective treatment can be provided on the basis of laboratory and clinical experience, even though the response to radioimmunotherapy varies depending on several factors, including tumor size, target density, tumor structure (e.g., liquid or solid, tumor microenvironment), the type of radiation administered, the heterogeneity of targeting at the microscopic level, and the ability to repair radiation damage.

A curative watershed for PRIT of solid tumors is the set of benchmarks that achieves a cumulative total of 8,000–10,000 cGy of absorbed radiation dose to individual tumor lesions while at the same time minimizing the dose to radiosensitive tissues, such as bone marrow (<150 cGy; TI, 40–100), small intestine (<250 cGy; TI, 40–60), and kidney (<1,500 cGy; TI, 6–10) (*1*). Two critical parameters to control for are tumor size and target density, because these directly influence tumor dose and TIs. We have called this collective of PRIT achievable properties the sweet spot. As shown in Tables 1 and 2, various forms of PRIT have the chance to achieve the sweet-spot high

tumor radiation dose and high TIs. Real-life examples from living systems support these ideas. These include the effectiveness of ^{131}I-NaI, a medium-energy β-emitter in certain thyroid cancers (*150*), and the cures achieved without histopathologic evidence of radiotoxicity in animal tumor models of human xenografts.

CONCLUSIONS AND OUTLOOK

PRIT is a form of targeted radiotherapy with internally administered radioemitters (radionuclide endotherapy, or unsealed radionuclides). As we have used the term here, an *antitumor vector* (e.g., Affibody, mAb, or nanoparticle) is the basis for tumor targeting and is modified to achieve desired properties of radionuclide capture during the targeting procedure. PRIT is a groundbreaking achievement because its components can be delivered in a time sequence that maximizes radiation to tumor while minimizing radiation to normal tissues. In this review, we have illustrated the current status of PRIT, with an emphasis on radiohapten capture (e.g., reversible binding using antihapten BsAb or biotin–streptavidin binding), bioorthogonal techniques (irreversible binding), and Affibody-PNA pretargeting that have shown high TIs in animal tumor models of human xenografts. In all 3 approaches, modified antitumor proteins provide the targeting specificity to tumor. As shown in Figure 1, other antitumor vectors and radionuclide forms for complementary radioligand capture, are proliferating.

During PRIT, the targeting vector and the radiohapten/carrier radiopharmacology are key parameters for high TI. Building on advances in protein engineering and mAb humanization, previous obstacles such as insufficient mAb/hapten affinity and immunogenicity can be overcome. Furthermore, we can more precisely balance the attributes of affinity, molecular size, and physicochemical properties of antibody-based carriers to improve tumor localization and penetration while limiting retention in normal tissues via rapid renal clearance. Also, with innovation in BsAb design, sufficient contrast and TI can be achieved without the aid of chase or CA, which would greatly simplify dosing to 2 steps and reagents.

Another exciting new frontier is high–linear-energy-transfer radiation, in which fewer quantitative guideposts for PRIT exist. There is an unmet need to define the dosimetry more completely, with α-emitters such as ^{225}Ac showing great promise (*151*). Work to estimate relative biologic effectiveness during PRIT with α-emitting radioisotopes is beginning (*152*).

In summary, pretargeting in nuclear medicine has achieved many milestones (Supplemental Table 1), including early-phase clinical testing (Supplemental Table 2). Pioneering clinical PRIT studies have demonstrated safety and that meaningful tumor doses can be achieved in select patients, but dosing is typically limited by insufficient TI, ADA, and the complexity of the approach. Still, clinical investigation of PRIT and radiotheranostics demonstrates increasing value for patient selection and treatment planning, permitting optimized reagent dosing during PRIT (Table 1). It is likely that individualized dosimetry will predict an optimized dose that will reduce the risk of underdosing tumors (leading to treatment failure) and overdosing normal tissues (leading to radiation toxicity).

REFERENCES

1. Larson SM, Carrasquillo JA, Cheung NK, Press OW. Radioimmunotherapy of human tumours. *Nat Rev Cancer.* 2015;15:347–360.
2. Wahl R. The success and failure of radioimmunotherapy for lymphoma [abstract]. *Endocrine Abstracts.* 2016;47:OC39.
3. Divgi C, Carrasquillo JA, Meredith R, et al. Overcoming barriers to radiopharmaceutical therapy (RPT): an overview from the NRG-NCI working group on dosimetry of radiopharmaceutical therapy. *Int J Radiat Oncol Biol Phys.* 2021;109:905–912.
4. Pouget JP, Constanzo J. Revisiting the radiobiology of targeted alpha therapy. *Front Med (Lausanne).* 2021;8:692436.
5. Kratochwil C, Bruchertseifer F, Giesel FL, et al. ^{225}Ac-PSMA-617 for PSMA-targeted alpha-radiation therapy of metastatic castration-resistant prostate cancer. *J Nucl Med.* 2016;57:1941–1944.
6. Tsai WK, Wu AM. Aligning physics and physiology: engineering antibodies for radionuclide delivery. *J Labelled Comp Radiopharm.* 2018;61:693–714.
7. Parakh S, Lee ST, Gan HK, Scott AM. Radiolabeled antibodies for cancer imaging and therapy. *Cancers (Basel).* 2022;14:1454.
8. Chomet M, van Dongen G, Vugts DJ. State of the art in radiolabeling of antibodies with common and uncommon radiometals for preclinical and clinical immuno-PET. *Bioconjug Chem.* 2021;32:1315–1330.
9. Moek KL, Giesen D, Kok IC, et al. Theranostics using antibodies and antibody-related therapeutics. *J Nucl Med.* 2017;58(suppl 2):83S–90S.
10. Sgouros G, Bodei L, McDevitt MR, Nedrow JR. Radiopharmaceutical therapy in cancer: clinical advances and challenges. *Nat Rev Drug Discov.* 2020;19:589–608.
11. Pressman D, Day ED, Blau M. The use of paired labeling in the determination of tumor-localizing antibodies. *Cancer Res.* 1957;17:845–850.
12. Bale WF, Spar IL, Goodland RL. Experimental radiation therapy of tumors with I-131-carrying antibodies to fibrin. *Cancer Res.* 1960;20:1488–1494.
13. Köhler G, Milstein C. Continuous cultures of fused cells secreting antibody of predefined specificity. *Nature.* 1975;256:495–497.
14. Goldenberg DM. Imaging and therapy of cancer with radiolabeled monoclonal antibodies. *Prog Clin Biol Res.* 1989;288:413–427.
15. Larson SM, Carrasquillo JA, Reynolds JC. Radioimmunodetection and radioimmunotherapy. *Cancer Invest.* 1984;2:363–381.
16. Kim EE, Deland FH, Casper S, Corgan RL, Primus FJ, Goldenberg DM. Radioimmunodetection of colorectal cancer. *Cancer.* 1980;45:1243–1247.
17. Reardan DT, Meares CF, Goodwin DA, et al. Antibodies against metal chelates. *Nature.* 1985;316:265–268.
18. Goodwin DA, Meares CF, McTigue M, David GS. Monoclonal antibody hapten radiopharmaceutical delivery. *Nucl Med Commun.* 1986;7:569–580.
19. Goodwin DA, Meares CF, McCall MJ, McTigue M, Chaovapong W. Pre-targeted immunoscintigraphy of murine tumors with indium-111-labeled bifunctional haptens. *J Nucl Med.* 1988;29:226–234.
20. Stickney DR, Anderson LD, Slater JB, et al. Bifunctional antibody: a binary radiopharmaceutical delivery system for imaging colorectal carcinoma. *Cancer Res.* 1991;51:6650–6655.
21. Hnatowich DJ, Virzi F, Rusckowski M. Investigations of avidin and biotin for imaging applications. *J Nucl Med.* 1987;28:1294–1302.
22. Pimm MV, Fells HF, Perkins AC, Baldwin RW. Iodine-131 and indium-111 labelled avidin and streptavidin for pre-targetted immunoscintigraphy with biotinylated anti-tumour monoclonal antibody. *Nucl Med Commun.* 1988;9:931–941.
23. Paganelli G, Riva P, Deleide G, et al. In vivo labelling of biotinylated monoclonal antibodies by radioactive avidin: a strategy to increase tumor radiolocalization. *Int J Cancer Suppl.* 1988;2:121–125.
24. Wilbur DS, Hamlin DK, Meyer DL, et al. Streptavidin in antibody pretargeting. 3. Comparison of biotin binding and tissue localization of 1,2-cyclohexanedione and succinic anhydride modified recombinant streptavidin. *Bioconjug Chem.* 2002;13:611–620.
25. Wilbur DS, Stayton PS, To R, et al. Streptavidin in antibody pretargeting: comparison of a recombinant streptavidin with two streptavidin mutant proteins and two commercially available streptavidin proteins. *Bioconjug Chem.* 1998;9:100–107.
26. Kalofonos HP, Rusckowski M, Siebecker DA, et al. Imaging of tumor in patients with indium-111-labeled biotin and streptavidin-conjugated antibodies: preliminary communication. *J Nucl Med.* 1990;31:1791–1796.
27. Paganelli G, Magnani P, Zito F, et al. Three-step monoclonal antibody tumor targeting in carcinoembryonic antigen-positive patients. *Cancer Res.* 1991;51:5960–5966.
28. Kraeber-Bodéré F, Rousseau C, Bodet-Milin C, et al. A pretargeting system for tumor PET imaging and radioimmunotherapy. *Front Pharmacol.* 2015;6:54.
29. Paganelli G, Chinol M, Grana C, et al. Therapy trials in cancer patients using an improved 3-step pretargeting approach. In: Bergmann H, Kroiss A, Sinzinger H, eds. *Radioactive Isotopes in Clinical Medicine and Research*: Springer; 1997: 513–517.
30. Papi S, Grana CG, Bartolomei M, et al. Pretargeted radioimmunotherapy in cancer: an overview. In: Hayat MA, ed. *Methods of Cancer Diagnosis, Therapy, and Prognosis: General Overviews, Head and Neck Cancer and Thyroid Cancer.* Springer; 2010:80–98.
31. Paganelli G, Grana C, Chinol M, et al. Antibody-guided three-step therapy for high grade glioma with yttrium-90 biotin. *Eur J Nucl Med.* 1999;26:348–357.

32. Goodwin DA, Meares CF, Osen M. Biological properties of biotin-chelate conjugates for pretargeted diagnosis and therapy with the avidin/biotin system. *J Nucl Med.* 1998;39:1813–1818.
33. Sharkey RM, Karacay H, Griffiths GL, et al. Development of a streptavidin-anti-carcinoembryonic antigen antibody, radiolabeled biotin pretargeting method for radioimmunotherapy of colorectal cancer: studies in a human colon cancer xenograft model. *Bioconjug Chem.* 1997;8:595–604.
34. Kuijpers WH, Bos ES, Kaspersen FM, Veeneman GH, van Boeckel CA. Specific recognition of antibody-oligonucleotide conjugates by radiolabeled antisense nucleotides: a novel approach for two-step radioimmunotherapy of cancer. *Bioconjug Chem.* 1993;4:94–102.
35. Rusckowski M, Qu T, Chang F, Hnatowich DJ. Pretargeting using peptide nucleic acid. *Cancer.* 1997;80:2699–2705.
36. Bos ES, Kuijpers WH, Meesters-Winters M, et al. In vitro evaluation of DNA-DNA hybridization as a two-step approach in radioimmunotherapy of cancer. *Cancer Res.* 1994;54:3479–3486.
37. Liu G. Use of morpholino oligomers for pretargeting. In: Moulton HM, Moulton JD, eds. *Morpholino Oligomers: Methods and Protocols.* Springer; 2017:161–179.
38. Axworthy D, Beaumier P, Bottino B, et al. Preclinical optimization of pretargeted radioimmunotherapy components: high efficiency, curative ^{90}Y delivery to mouse tumor xenografts. *Tumor Targeting.* 1996;2:156.
39. Axworthy DB, Reno JM, Hylarides MD, et al. Cure of human carcinoma xenografts by a single dose of pretargeted yttrium-90 with negligible toxicity. *Proc Natl Acad Sci USA.* 2000;97:1802–1807.
40. Murtha A, Weiden P, Knox S, et al. Phase I dose escalation trial of pretargeted radioimmunotherapy (PRIT) with ^{90}yttrium. *Proc Am Soc Clin Oncol* [abstract]. 1998;17:438.
41. Weiden PL, Breitz HB, Press O, et al. Pretargeted radioimmunotherapy (PRIT) for treatment of non-Hodgkin's lymphoma (NHL): initial phase I/II study results. *Cancer Biother Radiopharm.* 2000;15:15–29.
42. Breitz HB, Fisher DR, Goris ML, et al. Radiation absorbed dose estimation for ^{90}Y-DOTA-biotin with pretargeted NR-LU-10/streptavidin. *Cancer Biother Radiopharm.* 1999;14:381–395.
43. Knox SJ, Goris ML, Tempero M, et al. Phase II trial of yttrium-90-DOTA-biotin pretargeted by NR-LU-10 antibody/streptavidin in patients with metastatic colon cancer. *Clin Cancer Res.* 2000;6:406–414.
44. Lewis MR, Zhang J, Jia F, et al. Biological comparison of ^{149}Pm-, ^{166}Ho-, and ^{177}Lu-DOTA-biotin pretargeted by CC49 scFv-streptavidin fusion protein in xenograft-bearing nude mice. *Nucl Med Biol.* 2004;31:213–223.
45. Leichner PK, Akabani G, Colcher D, et al. Patient-specific dosimetry of indium-111- and yttrium-90-labeled monoclonal antibody CC49. *J Nucl Med.* 1997;38:512–516.
46. Shen S, Forero A, LoBuglio AF, et al. Patient-specific dosimetry of pretargeted radioimmunotherapy using CC49 fusion protein in patients with gastrointestinal malignancies. *J Nucl Med.* 2005;46:642–651.
47. Förster GJ, Santos EB, Smith-Jones PM, Zanzonico P, Larson SM. Pretargeted radioimmunotherapy with a single-chain antibody/streptavidin construct and radiolabeled DOTA-biotin: strategies for reduction of the renal dose. *J Nucl Med.* 2006;47:140–149.
48. Yao Z, Zhang M, Garmestani K, et al. Pretargeted alpha emitting radioimmunotherapy using ^{213}Bi 1,4,7,10-tetraazacyclododecane-*N,N′,N′′,N′′′*-tetraacetic acid-biotin. *Clin Cancer Res.* 2004;10:3137–3146.
49. Yao Z, Zhang M, Axworthy DB, et al. Radioimmunotherapy of A431 xenografted mice with pretargeted B3 antibody-streptavidin and ^{90}Y-labeled 1,4,7,10-tetraazacyclododecane-*N,N′,N′′,N′′′*-tetraacetic acid (DOTA)-biotin. *Cancer Res.* 2002;62:5755–5760.
50. Sato N, Hassan R, Axworthy DB, et al. Pretargeted radioimmunotherapy of mesothelin-expressing cancer using a tetravalent single-chain Fv-streptavidin fusion protein. *J Nucl Med.* 2005;46:1201–1209.
51. Cheung NK, Modak S, Lin Y, et al. Single-chain Fv-streptavidin substantially improved therapeutic index in multistep targeting directed at disialoganglioside GD2. *J Nucl Med.* 2004;45:867–877.
52. Press OW, Appelbaum F, Martin P, et al. Phase II trial of ^{131}I-B1 (anti-CD20) antibody therapy with autologous stem cell transplantation for relapsed B cell lymphomas. *Lancet.* 1995;346:336–340.
53. Witzig TE, Gordon LI, Cabanillas F, et al. Randomized controlled trial of yttrium-90-labeled ibritumomab tiuxetan radioimmunotherapy versus rituximab immunotherapy for patients with relapsed or refractory low-grade, follicular, or transformed B-cell non-Hodgkin's lymphoma. *J Clin Oncol.* 2002;20:2453–2463.
54. Press OW, Corcoran M, Subbiah K, et al. A comparative evaluation of conventional and pretargeted radioimmunotherapy of CD20-expressing lymphoma xenografts. *Blood.* 2001;98:2535–2543.
55. Breitz HB, Weiden PL, Beaumier PL, et al. Clinical optimization of pretargeted radioimmunotherapy with antibody-streptavidin conjugate and ^{90}Y-DOTA-biotin. *J Nucl Med.* 2000;41:131–140.
56. Schultz J, Lin Y, Sanderson J, et al. A tetravalent single-chain antibody-streptavidin fusion protein for pretargeted lymphoma therapy. *Cancer Res.* 2000;60:6663–6669.
57. Forero A, Weiden PL, Vose JM, et al. Phase 1 trial of a novel anti-CD20 fusion protein in pretargeted radioimmunotherapy for B-cell non-Hodgkin lymphoma. *Blood.* 2004;104:227–236.
58. Zhang M, Zhang Z, Garmestani K, et al. Pretarget radiotherapy with an anti-CD25 antibody-streptavidin fusion protein was effective in therapy of leukemia/lymphoma xenografts. *Proc Natl Acad Sci USA.* 2003;100:1891–1895.
59. Pagel JM, Hedin N, Subbiah K, et al. Comparison of anti-CD20 and anti-CD45 antibodies for conventional and pretargeted radioimmunotherapy of B-cell lymphomas. *Blood.* 2003;101:2340–2348.
60. Pantelias A, Pagel JM, Hedin N, et al. Comparative biodistributions of pretargeted radioimmunoconjugates targeting CD20, CD22, and DR molecules on human B-cell lymphomas. *Blood.* 2007;109:4980–4987.
61. Le Doussal JM, Martin M, Gautherot E, Delaage M, Barbet J. In vitro and in vivo targeting of radiolabeled monovalent and divalent haptens with dual specificity monoclonal antibody conjugates: enhanced divalent hapten affinity for cell-bound antibody conjugate. *J Nucl Med.* 1989;30:1358–1366.
62. Goodwin DA, Meares CF, Watanabe N, et al. Pharmacokinetics of pretargeted monoclonal antibody 2D12.5 and ^{88}Y-Janus-2-(p-nitrobenzyl)-1,4,7,10-tetraazacyclododecanetetraacetic acid (DOTA) in BALB/c mice with KHJJ mouse adenocarcinoma: a model for ^{90}Y radioimmunotherapy. *Cancer Res.* 1994;54:5937–5946.
63. Le Doussal JM, Chetanneau A, Gruaz-Guyon A, et al. Bispecific monoclonal antibody-mediated targeting of an indium-111-labeled DTPA dimer to primary colorectal tumors: pharmacokinetics, biodistribution, scintigraphy and immune response. *J Nucl Med.* 1993;34:1662–1671.
64. Peltier P, Curtet C, Chatal JF, et al. Radioimmunodetection of medullary thyroid cancer using a bispecific anti-CEA/anti-indium-DTPA antibody and an indium-111-labeled DTPA dimer. *J Nucl Med.* 1993;34:1267–1273.
65. Barbet J, Peltier P, Bardet S, et al. Radioimmunodetection of medullary thyroid carcinoma using indium-111 bivalent hapten and anti-CEA × anti-DTPA-indium bispecific antibody. *J Nucl Med.* 1998;39:1172–1178.
66. Vuillez JP, Moro D, Brichon PY, et al. Two-step immunoscintigraphy for non-small-cell lung cancer staging using a bispecific anti-CEA/anti-indium-DTPA antibody and an indium-111-labeled DTPA dimer. *J Nucl Med.* 1997;38:507–511.
67. Bardiès M, Bardet S, Faivre-Chauvet A, et al. Bispecific antibody and iodine-131-labeled bivalent hapten dosimetry in patients with medullary thyroid or small-cell lung cancer. *J Nucl Med.* 1996;37:1853–1859.
68. Barbet J, Kraeber-Bodere F, Vuillez JP, Gautherot E, Rouvier E, Chatal JF. Pretargeting with the affinity enhancement system for radioimmunotherapy. *Cancer Biother Radiopharm.* 1999;14:153–166.
69. Karacay H, McBride W, Griffiths G, et al. Experimental pretargeting studies of cancer with a humanized anti-CEA× murine anti-[In-DTPA] bispecific antibody construct and a ^{99m}Tc-/^{188}Re-labeled peptide. *Bioconjug Chem.* 2000;11:842–854.
70. Kraeber-Bodéré F, Faivre-Chauvet A, Saï-Maurel C, et al. Bispecific antibody and bivalent hapten radioimmunotherapy in CEA-producing medullary thyroid cancer xenograft. *J Nucl Med.* 1999;40:198–204.
71. Kraeber-Bodéré F, Bardet S, Hoefnagel CA, et al. Radioimmunotherapy in medullary thyroid cancer using bispecific antibody and iodine 131-labeled bivalent hapten: preliminary results of a phase I/II clinical trial. *Clin Cancer Res.* 1999;5(suppl):3190s–3198s.
72. Vuillez J-P, Kraeber-Bodéré F, Moro D, et al. Radioimmunotherapy of small cell lung carcinoma with the two-step method using a bispecific anti-carcinoembryonic antigen/anti-diethylenetriaminepentaacetic acid (DTPA) antibody and iodine-131 Di-DTPA hapten: results of a phase I/II trial. *Clin Cancer Res.* 1999;5(suppl):3259s–3267s.
73. Kraeber-Bodéré F, Faivre-Chauvet A, Ferrer L, et al. Pharmacokinetics and dosimetry studies for optimization of anti-carcinoembryonic antigen × anti-hapten bispecific antibody-mediated pretargeting of iodine-131-labeled hapten in a phase I radioimmunotherapy trial. *Clin Cancer Res.* 2003;9:3973S–3981S.
74. Kraeber-Bodéré F, Rousseau C, Bodet-Milin C, et al. Targeting, toxicity, and efficacy of 2-step, pretargeted radioimmunotherapy using a chimeric bispecific antibody and ^{131}I-labeled bivalent hapten in a phase I optimization clinical trial. *J Nucl Med.* 2006;47:247–255.
75. Chatal J-F, Campion L, Kraeber-Bodéré F, et al. Survival improvement in patients with medullary thyroid carcinoma who undergo pretargeted anti-carcinoembryonic-antigen radioimmunotherapy: a collaborative study with the French Endocrine Tumor Group. *J Clin Oncol.* 2006;24:1705–1711.
76. Boerman OC, Kranenborg MH, Oosterwijk E, et al. Pretargeting of renal cell carcinoma: improved tumor targeting with a bivalent chelate. *Cancer Res.* 1999;59:4400–4405.
77. van Schaijk FG, Oosterwijk E, Molkenboer-Kuenen JD, et al. Pretargeting with bispecific anti-renal cell carcinoma x anti-DTPA(In) antibody in 3 RCC models. *J Nucl Med.* 2005;46:495–501.

78. van Schaijk FG, Broekema M, Oosterwijk E, et al. Residualizing iodine markedly improved tumor targeting using bispecific antibody-based pretargeting. *J Nucl Med.* 2005;46:1016–1022.
79. van Schaijk FG, Oosterwijk E, Soede AC, et al. Pretargeting of carcinoembryonic antigen–expressing tumors with a biologically produced bispecific anticarcinoembryonic antigen × anti-indium–labeled diethylenetriaminepentaacetic acid antibody. *Clin Cancer Res.* 2005;11:7130s–7136s.
80. Sharkey RM, Goldenberg DM. Advances in radioimmunotherapy in the age of molecular engineering and pretargeting. *Cancer Invest.* 2006;24:82–97.
81. Feng X, Pak R, Kroger L, et al. New anti-Cu-TETA and anti-Y-DOTA monoclonal antibodies for potential use in the pre-targeted delivery of radiopharmaceuticals to tumor. *Hybridoma.* 1998;17:125–132.
82. Janevik-Ivanovska E, Gautherot E, Hillairet de Boisferon M, et al. Bivalent hapten-bearing peptides designed for iodine-131 pretargeted radioimmunotherapy. *Bioconjug Chem.* 1997;8:526–533.
83. Karacay H, Sharkey R, McBride W, et al. Pretargeting for cancer radioimmunotherapy with bispecific antibodies: role of the bispecific antibody's valency for the tumor target antigen. *Bioconjug Chem.* 2002;13:1054–1070.
84. Sharkey RM, McBride WJ, Karacay H, et al. A universal pretargeting system for cancer detection and therapy using bispecific antibody. *Cancer Res.* 2003;63:354–363.
85. Sharkey RM, Cardillo TM, Rossi EA, et al. Signal amplification in molecular imaging by pretargeting a multivalent, bispecific antibody. *Nat Med.* 2005;11:1250–1255.
86. McBride WJ, Zanzonico P, Sharkey RM, et al. Bispecific antibody pretargeting PET (immunoPET) with an ^{124}I-labeled hapten-peptide. *J Nucl Med.* 2006;47:1678–1688.
87. Rossi EA, Sharkey RM, McBride W, et al. Development of new multivalent-bispecific agents for pretargeting tumor localization and therapy. *Clin Cancer Res.* 2003;9:3886S–3896S.
88. Chang C-H, Rossi EA, Goldenberg DM. The dock and lock method: a novel platform technology for building multivalent, multifunctional structures of defined composition with retained bioactivity. *Clin Cancer Res.* 2007;13:5586s–5591s.
89. Goldenberg DM, Rossi EA, Sharkey RM, McBride WJ, Chang CH. Multifunctional antibodies by the dock-and-lock method for improved cancer imaging and therapy by pretargeting. *J Nucl Med.* 2008;49:158–163.
90. Goldenberg DM, Chang CH, Rossi EA, McBride JW, Sharkey RM. Pretargeted molecular imaging and radioimmunotherapy. *Theranostics.* 2012;2:523–540.
91. Frampas E, Maurel C, Saëc R-L, et al. Pretargeted radioimmunotherapy of colorectal cancer metastases: models and pharmacokinetics predict influence of the physical and radiochemical properties of the radionuclide. *Eur J Nucl Med Mol Imaging.* 2011;38:2153–2164.
92. Karacay H, Sharkey RM, Gold DV, et al. Pretargeted radioimmunotherapy of pancreatic cancer xenografts: TF10–^{90}Y-IMP-288 alone and combined with gemcitabine. *J Nucl Med.* 2009;50:2008–2016.
93. Karacay H, Brard P-Y, Sharkey RM, et al. Therapeutic advantage of pretargeted radioimmunotherapy using a recombinant bispecific antibody in a human colon cancer xenograft. *Clin Cancer Res.* 2005;11:7879–7885.
94. Sharkey RM, Rossi EA, McBride WJ, Chang C-H, Goldenberg DM. Recombinant bispecific monoclonal antibodies prepared by the dock-and-lock strategy for pretargeted radioimmunotherapy. *Semin Nucl Med.* 2010;40:190–203.
95. Mawad R, Gooley T, Rajendran JG, et al. Pretargeted radioimmunotherapy using an anti-CD45 antibody-streptavidin conjugate and radiolabeled DOTA-biotin in patients with high-risk acute leukemia or myelodysplastic syndrome undergoing allogeneic hematopoietic cell transplantation [abstract]. *Biol Blood Marrow Transplant.* 2013;19(suppl):S123–S124.
96. Paganelli G, Ferrari M, Ravasi L, et al. Intraoperative avidination for radionuclide therapy: a prospective new development to accelerate radiotherapy in breast cancer. *Clin Cancer Res.* 2007;13:5646s–5651s.
97. Petronzelli F, Pelliccia A, Anastasi AM, et al. Therapeutic use of avidin is not hampered by antiavidin antibodies in humans. *Cancer Biother Radiopharm.* 2010;25:563–570.
98. De Santis R, Leoni B, Rosi A, et al. AvidinOX for highly efficient tissue-pretargeted radionuclide therapy. *Cancer Biother Radiopharm.* 2010;25:143–148.
99. Albertoni C, Leoni B, Rosi A, et al. Radionuclide therapy of unresectable tumors with AvidinOX and ^{90}Y-biotinDOTA: tongue cancer paradigm. *Cancer Biother Radiopharm.* 2015;30:291–298.
100. De Santis R, Leoni B, Rosi A, et al. AvidinOX for highly efficient tissue-pretargeted radionuclide therapy. *Cancer Biother Radiopharm.* 2010;25:143–148.
101. Vesci L, Carollo V, Rosi A, De Santis R. Therapeutic efficacy of intra-tumor AvidinOX and low systemic dose biotinylated cetuximab, with and without cisplatin, in an orthotopic model of head and neck cancer. *Oncol Lett.* 2019;17:3529–3536.
102. Frost SH, Bäck T, Chouin N, et al. Comparison of ^{211}At-PRIT and ^{211}At-RIT of ovarian microtumors in a nude mouse model. *Cancer Biother Radiopharm.* 2013;28:108–114.
103. Frost SH, Frayo SL, Miller BW, et al. Comparative efficacy of ^{177}Lu and ^{90}Y for anti-CD20 pretargeted radioimmunotherapy in murine lymphoma xenograft models. *PLoS One.* 2015;10:e0120561.
104. Green DJ, Frayo SL, Lin Y, et al. Comparative analysis of bispecific antibody and streptavidin-targeted radioimmunotherapy for B-cell cancers. *Cancer Res.* 2016;76:6669–6679.
105. Green DJ, Press OW. Whither radioimmunotherapy: to be or not to be? *Cancer Res.* 2017;77:2191–2196.
106. Lütje S, Rijpkema M, Goldenberg DM, et al. Pretargeted dual-modality immuno-SPECT and near-infrared fluorescence imaging for image-guided surgery of prostate cancer. *Cancer Res.* 2014;74:6216–6223.
107. Heskamp S, Hernandez R, Molkenboer-Kuenen JDM, et al. α- versus β-emitting radionuclides for pretargeted radioimmunotherapy of carcinoembryonic antigen-expressing human colon cancer xenografts. *J Nucl Med.* 2017;58:926–933.
108. Schoffelen R, Boerman OC, Goldenberg DM, et al. Development of an imaging-guided CEA-pretargeted radionuclide treatment of advanced colorectal cancer: first clinical results. *Br J Cancer.* 2013;109:934–942.
109. Schoffelen R, Woliner-van der Weg W, Visser EP, et al. Predictive patient-specific dosimetry and individualized dosing of pretargeted radioimmunotherapy in patients with advanced colorectal cancer. *Eur J Nucl Med Mol Imaging.* 2014;41:1593–1602.
110. Woliner-van der Weg W, Schoffelen R, Hobbs RF, et al. Tumor and red bone marrow dosimetry: comparison of methods for prospective treatment planning in pretargeted radioimmunotherapy. *EJNMMI Phys.* 2015;2:5.
111. Bodet-Milin C, Ferrer L, Rauscher A, et al. Pharmacokinetics and dosimetry studies for optimization of pretargeted radioimmunotherapy in CEA-expressing advanced lung cancer patients. *Front Med (Lausanne).* 2015;2:84.
112. Bodet-Milin C, Faivre-Chauvet A, Carlier T, et al. Immuno-PET using anticarcinoembryonic antigen bispecific antibody and ^{68}Ga-labeled peptide in metastatic medullary thyroid carcinoma: clinical optimization of the pretargeting parameters in a first-in-human trial. *J Nucl Med.* 2016;57:1505–1511.
113. Touchefeu Y, Bailly C, Frampas E, et al. Promising clinical performance of pretargeted immuno-PET with anti-CEA bispecific antibody and gallium-68-labelled IMP-288 peptide for imaging colorectal cancer metastases: a pilot study. *Eur J Nucl Med Mol Imaging.* 2021;48:874–882.
114. Rousseau C, Goldenberg DM, Colombie M, et al. initial clinical results of a novel immuno-PET theranostic probe in human epidermal growth factor receptor 2-negative breast cancer. *J Nucl Med.* 2020;61:1205–1211.
115. Bodet-Milin C, Faivre-Chauvet A, Carlier T, et al. Anti-CEA pretargeted immuno-PET shows higher sensitivity than DOPA PET/CT in detecting relapsing metastatic medullary thyroid carcinoma: post hoc analysis of the iPET-MTC study. *J Nucl Med.* 2021;62:1221–1227.
116. Orcutt KD, Slusarczyk AL, Cieslewicz M, et al. Engineering an antibody with picomolar affinity to DOTA chelates of multiple radionuclides for pretargeted radioimmunotherapy and imaging. *Nucl Med Biol.* 2011;38:223–233.
117. Orcutt KD, Ackerman ME, Cieslewicz M, et al. A modular IgG-scFv bispecific antibody topology. *Protein Eng Des Sel.* 2010;23:221–228.
118. Orcutt KD, Nasr KA, Whitehead DG, Frangioni JV, Wittrup KD. Biodistribution and clearance of small molecule hapten chelates for pretargeted radioimmunotherapy. *Mol Imaging Biol.* 2011;13:215–221.
119. Orcutt KD, Rhoden JJ, Ruiz-Yi B, Frangioni JV, Wittrup KD. Effect of small-molecule-binding affinity on tumor uptake in vivo: a systematic study using a pretargeted bispecific antibody. *Mol Cancer Ther.* 2012;11:1365–1372.
120. Cheal SM, Xu H, Guo HF, Zanzonico PB, Larson SM, Cheung NK. Preclinical evaluation of multistep targeting of diasialoganglioside GD2 using an IgG-scFv bispecific antibody with high affinity for GD2 and DOTA metal complex. *Mol Cancer Ther.* 2014;13:1803–1812.
121. Cheal SM, Xu H, Guo HF, et al. Theranostic pretargeted radioimmunotherapy of colorectal cancer xenografts in mice using picomolar affinity ^{86}Y- or ^{177}Lu-DOTA-Bn binding scFv C825/GPA33 IgG bispecific immunoconjugates. *Eur J Nucl Med Mol Imaging.* 2016;43:925–937.
122. Cheal SM, Xu H, Guo HF, et al. Theranostic pretargeted radioimmunotherapy of internalizing solid tumor antigens in human tumor xenografts in mice: curative treatment of HER2-positive breast carcinoma. *Theranostics.* 2018;8:5106–5125.
123. Cheal SM, McDevitt MR, Santich BH, et al. Alpha radioimmunotherapy using ^{225}Ac-proteus-DOTA for solid tumors: safety at curative doses. *Theranostics.* 2020;10:11359–11375.
124. Cheal SM, Patel M, Yang G, et al. An *N*-acetylgalactosamino dendron-clearing agent for high-therapeutic-index DOTA-hapten pretargeted radioimmunotherapy. *Bioconjug Chem.* 2020;31:501–506.
125. Orozco JJ, Kenoyer AL, Lin Y, et al. Therapy of myeloid leukemia using novel bispecific fusion proteins targeting CD45 and ^{90}Y-DOTA. *Mol Cancer Ther.* 2020;19:2575–2584.

126. Green DJ, O'Steen S, Lin Y, et al. CD38-bispecific antibody pretargeted radioimmunotherapy for multiple myeloma and other B-cell malignancies. *Blood.* 2018; 131:611–620.
127. Santich BH, Cheal SM, Ahmed M, et al. A self-assembling and disassembling (SADA) bispecific antibody (BsAb) platform for curative two-step pretargeted radioimmunotherapy. *Clin Cancer Res.* 2021;27:532–541.
128. Torgue J, Jurek P, Rojas-Quijano F, et al., inventors; Hoffmann-La Roche Inc., Orano Med SAS, assignees. Antibodies for chelated radionuclides and clearing agents. World Intellectual Property Organization patent WO2019202399A8. December 12, 2019.
129. Frost S, Pichard A, Haas A, et al. Preclinical evaluation of CEA-PRIT, a novel pretargeted alpha therapy regimen for treatment of CEA-positive tumours with Pb-212 [abstract]. *Eur J Nucl Med Mol Imaging.* 2019;46(suppl):S56–S57.
130. Sörensen J, Sandberg D, Sandstrom M, et al. First-in-human molecular imaging of HER2 expression in breast cancer metastases using the ^{111}In-ABY-025 affibody molecule. *J Nucl Med.* 2014;55:730–735.
131. Tolmachev V, Orlova A, Pehrson R, et al. Radionuclide therapy of HER2-positive microxenografts using a ^{177}Lu-labeled HER2-specific Affibody molecule. *Cancer Res.* 2007;67:2773–2782.
132. Westerlund K, Altai M, Mitran B, et al. Radionuclide therapy of HER2-expressing human xenografts using affibody-based peptide nucleic acid-mediated pretargeting: in vivo proof of principle. *J Nucl Med.* 2018;59:1092–1098.
133. Altai M, Perols A, Tsourma M, et al. Feasibility of affibody-based bioorthogonal chemistry-mediated radionuclide pretargeting. *J Nucl Med.* 2016;57:431–436.
134. Krebs S, Ahad A, Carter LM, et al. Antibody with infinite affinity for in vivo tracking of genetically engineered lymphocytes. *J Nucl Med.* 2018;59:1894–1900.
135. Day JJ, Marquez BV, Beck HE, Aweda TA, Gawande PD, Meares CF. Chemically modified antibodies as diagnostic imaging agents. *Curr Opin Chem Biol.* 2010;14:803–809.
136. Scinto SL, Bilodeau DA, Hincapie R, et al. Bioorthogonal chemistry. *Nat Rev Methods Primers.* 2021;1:30.
137. Rossin R, Verkerk PR, van den Bosch SM, et al. In vivo chemistry for pretargeted tumor imaging in live mice. *Angew Chem Int Ed Engl.* 2010;49:3375–3378.
138. Rondon A, Degoul F. Antibody pretargeting based on bioorthogonal click chemistry for cancer imaging and targeted radionuclide therapy. *Bioconjug Chem.* 2020; 31:159–173.
139. Shah MA, Zhang X, Rossin R, et al. Metal-free cycloaddition chemistry driven pretargeted radioimmunotherapy using alpha-particle radiation. *Bioconjug Chem.* 2017;28:3007–3015.
140. Houghton JL, Membreno R, Abdel-Atti D, et al. Establishment of the in vivo efficacy of pretargeted radioimmunotherapy utilizing inverse electron demand Diels-Alder click chemistry. *Mol Cancer Ther.* 2017;16:124–133.
141. Membreno R, Cook BE, Fung K, Lewis JS, Zeglis BM. Click-mediated pretargeted radioimmunotherapy of colorectal carcinoma. *Mol Pharm.* 2018;15: 1729–1734.
142. Poty S, Carter LM, Mandleywala K, et al. Leveraging bioorthogonal click chemistry to improve ^{225}Ac-radioimmunotherapy of pancreatic ductal adenocarcinoma. *Clin Cancer Res.* 2019;25:868–880.
143. Membreno R, Keinänen OM, Cook BE, et al. Toward the optimization of click-mediated pretargeted radioimmunotherapy. *Mol Pharm.* 2019;16:2259–2263.
144. Keinänen O, Fung K, Brennan JM, et al. Harnessing ^{64}Cu/^{67}Cu for a theranostic approach to pretargeted radioimmunotherapy. *Proc Natl Acad Sci USA.* 2020; 117:28316–28327.
145. Strebl MG, Yang J, Isaacs L, Hooker JM. Adamantane/cucurbituril: a potential pretargeted imaging strategy in immuno-PET. *Mol Imaging.* 2018;17:1536012118799838.
146. Au KM, Tripathy A, Lin CP, et al. Bespoke pretargeted nanoradioimmunotherapy for the treatment of non-Hodgkin lymphoma. *ACS Nano.* 2018;12:1544–1563.
147. Huang Z, Hu Y, Yang Y, Huang W, Wang Y, Ye D. Recent advances in pretargeted imaging of tumors in vivo. *Analysis Sensing.* April 21, 2022 [Epub ahead of print].
148. Stéen EJL, Jørgensen JT, Denk C, et al. Lipophilicity and click reactivity determine the performance of bioorthogonal tetrazine tools in pretargeted in vivo chemistry. *ACS Pharmacol Transl Sci.* 2021;4:824–833.
149. Jallinoja VIJ, Houghton JL. Current landscape in clinical pretargeted radioimmunoimaging and therapy. *J Nucl Med.* 2021;62:1200–1206.
150. Maxon HR, Thomas SR, Samaratunga RC. Dosimetric considerations in the radioiodine treatment of macrometastases and micrometastases from differentiated thyroid cancer. *Thyroid.* 1997;7:183–187.
151. Kratochwil C, Haberkorn U, Giesel FL. ^{225}Ac-PSMA-617 for therapy of prostate cancer. *Semin Nucl Med.* 2020;50:133–140.
152. Poty S, Mandleywala K, O'Neill E, Knight JC, Cornelissen B, Lewis JS. ^{89}Zr-PET imaging of DNA double-strand breaks for the early monitoring of response following α- and β-particle radioimmunotherapy in a mouse model of pancreatic ductal adenocarcinoma. *Theranostics.* 2020;10:5802–5814.
153. Robillard MS, Rossin R. In-vivo chemistry for pretargeted tumor imaging and therapy in mice. *Medicamundi.* 2010;54:55–62.
154. Sharkey RM, Karacay H, Litwin S, et al. Improved therapeutic results by pretargeted radioimmunotherapy of non-Hodgkin's lymphoma with a new recombinant, trivalent, anti-CD20, bispecific antibody. *Cancer Res.* 2008;68:5282–5290.
155. Tano H, Oroujeni M, Vorobyeva A, et al. Comparative evaluation of novel ^{177}Lu-labeled PNA probes for affibody-mediated PNA-based pretargeting. *Cancers (Basel).* 2021;13:500.
156. Altai M, Strand J, Rosik D, et al. Influence of nuclides and chelators on imaging using affibody molecules: comparative evaluation of recombinant affibody molecules site-specifically labeled with ^{68}Ga and ^{111}In via maleimido derivatives of DOTA and NODAGA. *Bioconjug Chem.* 2013;24:1102–1109.
157. Hosono M, Hosono MN, Kraeber-Bodéré F, Devys A. Biodistribution and dosimetric study in medullary thyroid cancer xenograft using bispecific antibody and iodine-125-labeled bivalent hapten. *J Nucl Med.* 1998;39:1608–1613.
158. Feijtel D, Doeswijk GN, Verkaik NS, et al. Inter and intra-tumor somatostatin receptor 2 heterogeneity influences peptide receptor radionuclide therapy response. *Theranostics.* 2021;11:491–505.